3-1978

Negative Ion Resonances in the Fluorobenzenes and Biphenyl

John Ronald Frazier
University of Tennessee, Knoxville

To the Graduate Council:

I am submitting herewith a dissertation written by John Ronald Frazier entitled "Negative Ion Resonances in the Fluorobenzenes and Biphenyl." I have examined the final electronic copy of this dissertation for form and content and recommend that it be accepted in partial fulfillment of the requirements for the degree of Doctor of Philosophy, with a major in Physics.

Loucas G. Christophorou, Major Professor

We have read this dissertation and recommend its acceptance:

Robert J. Lovell, John Creely, Harold Schweinler, R. O. Barnawell, R. Y. Pai

Accepted for the Council:

Carolyn R. Hodges

Vice Provost and Dean of the Graduate School

(Original signatures are on file with official student records.)

To the Graduate Council:

I am submitting herewith a dissertation written by John Ronald Frazier entitled "Negative Ion Resonances in the Fluorobenzenes and Biphenyl." I recommend that it be accepted in partial fulfillment of the requirements for the degree of Doctor of Philosophy, with a major in Physics.

Loucas G. Christophorou

Loucas G. Christophorou, Major Professor

We have read this dissertation
and recommend its acceptance:

Accepted for the Council:

L. G. Evans

Vice Chancellor
Graduate Studies and Research

NEGATIVE ION RESONANCES IN THE FLUOROBENZENES AND BIPHENYL

A Dissertation

Presented for the

Doctor of Philosophy

Degree

The University of Tennessee, Knoxville

John Ronald Frazier

March 1978

ACKNOWLEDGMENTS

The author wishes to express his gratitude to the many persons who have contributed to his educational experience. While it is impossible to acknowledge all of those persons, there are certain individuals who have been invaluable during the performance of this research.

D. V. Maxey, J. G. Carter, and H. L. Barnawell of the Health and Safety Research Division of Oak Ridge National Laboratory provided experimental and technical expertise during all stages of this research.

The author wishes to thank Drs. H. C. Schweinler, J. D. Allen, K. Siamos, and R. Y. Pai for many enlivened discussions of the present experiment.

Appreciation is expressed to Dr. L. G. Christophorou who provided encouragement and patience to the author during this research.

Financial assistance was provided, during the author's first year of graduate study, by a Special Fellowship in Radiation Science and Protection from Oak Ridge Associated Universities. The remaining years of graduate study were supported primarily by a Graduate Teaching Assistantship from the University of Tennessee.

The author wishes to recognize the work of his wife, Patti, who typed all drafts of this dissertation. Her encouragement, support, and concern were immeasurable during the author's graduate education.

ABSTRACT

An electron transmission technique has been employed to determine the positions of the three π-negative ion states (configurations $\pi_1^2\pi_2^2\pi_3^2\pi_4^1$, $\pi_1^2\pi_2^2\pi_3^2\pi_5^1$, and $\pi_1^2\pi_2^2\pi_3^2\pi_6^1$) of fluorobenzenes in the vapor phase. These are 1.13 (1.35), 1.13 (1.35), (4.80) eV for benzene (B); 0.82 (0.91), (1.40), (4.66) eV for fluorobenzene (FB); 0.53 (0.62), (1.41), (4.51) eV for p-difluorobenzene (p-DFB); (0.77), (0.77), (4.48) eV for 1,3,5-trifluorobenzene (1,3,5-TFB); 0.34 (0.50), (1.29), (4.51) eV for 2,3,5,6-tetrafluorobenzene (2,3,5,6-TFB); ($\sim$0.4), (1.19), (4.53) eV for pentafluorobenzene (PFB); and (0.42), (0.42), (4.50) eV for hexafluorobenzene (HFB). The numbers in parentheses are the vertical attachment energies (VAE's) and those not in parentheses are the 0$\rightarrow$0 transitions. On the basis of these data, the first π-electron affinities (EA) of the isolated molecules of these compounds are equal to -1.13, -0.82, -0.53, $\geq$ -0.77, -0.34, $\geq$ -0.4(?), $\geq$ -0.42 for B, FB, p-DFB, 1,3,5-TFB, 2,3,5,6-TFB, PFB, and HFB, respectively. The present results, therefore, suggest that the π-electron affinity of C_6F_6 is < 0.0 eV, although C_6F_6 is known to have a positive (+1.8 eV) EA and although the parent ion, $C_6F_6^{-*}$, is known to form with a very large electron attachment cross section at $\sim$0.0 eV and to be long lived ($\sim$12 μsec). These findings can be reconciled by assuming that the lowest negative ion state of HFB is not the π_4,π_5 degenerate state reached in the present electron scattering

experiments but that it is possibly another negative ion state associated with either a σ orbital or a molecular geometrical distortion upon negative ion formation.

Electron transmission spectra of biphenyl ($C_{12}H_{10}$) in the vapor phase reveal four π-negative ion states for electron energies less than 3.0 eV. These are centered at 0.44, 0.93, 1.27, and 1.88 eV and correspond to VAE's of -0.44, -0.93, -1.27, and -1.88 eV, respectively. These are assigned to electron capture into the π_7, π_8, π_9, and π_{10} orbitals, respectively. Comparison between benzene VAE's and biphenyl VAE's revealed a strong π-π interaction between the benzene rings.

TABLE OF CONTENTS

LIST OF TABLES

LIST OF FIGURES

FIGURE PAGE

CHAPTER I

INTRODUCTION

I. IMPORTANCE OF NEGATIVE IONS

A negative ion is an atom or a molecule with a net negative charge. Such ions are found in all phases of matter as well as in terrestrial and celestial locations. In many branches of science and engineering the importance of negative ions has been realized for several years. Investigations of their formation and decay as well as of their basic and practical significance continue.

Electrical engineers have found that certain electron attaching gases are capable of withstanding very strong electric fields without electrical breakdown. The high dielectric strengths of certain gases surely play a major role in the design of more efficient power transmission systems.

In the field of astrophysics negative ions play an important role in determining the spectral distribution of visible light from the sun. Equally as important is the role that negative ion formation, with the ensuing autodetachment, serves in modern radio and television communications.

The existence of negative ions in biological systems is one of much conjecture and speculation. As ionizing radiation penetrates living systems, large numbers of low-energy electrons are formed within individual cells. The

finite probability that negative ions will be formed (e.g. via electron attachment) in these biosystems suggests possible pathways for "damage" to occur. One possibility would be molecular dissociation of the negative ion with ensuing biochemical reactions. Much research is needed in this area.

Theoretical chemists who subscribe to the semi-empirical approach for molecular bonding models make use of experimentally obtained information of negative ions. A stable molecular negative ion would indicate an additional bound molecular orbital and the orbital binding energy would be positive. A molecular negative ion which is unstable with respect to decay would indicate either a vibrationally excited state of a (normally) bound system or an unbound molecular orbital state. The semi-empirical treatment of a bonding model correlates the experimentally obtained energies of negative ion formation with the values obtained from quantum mechanical calculations. The semi-empiricist works toward a reconciliation of existing bond theory with available experimental data.

Several authors have devoted much attention to negative ions and their importance (e.g., Massey, 1950; McDaniel, 1964; Hasted, 1964; Christophorou, 1971; and Massey, 1976). The more recent book by Massey (1976) is a comprehensive treatment of negative ions: their formation, interactions, lifetimes and decay channels.

II. LOW-ENERGY ELECTRON-MOLECULE INTERACTIONS

Throughout the present work the term "low-energy electrons" refers to electrons with kinetic energy between thermal energies and 7.50 electron volts (eV). Electrons in this energy range have a speed such that the normal transit time of the electron over the molecular dimensions is less than the vibrational period of the molecule. Electrons with these energies have insufficient energy to ionize the molecules studied. Such electrons may lose energy via direct elastic and inelastic collisions, indirectly via negative ion resonance states, and also via the various electron attachment processes. It has been shown (see for example, Christophorou, 1977) that, of the above mentioned modes, indirect electron scattering at low energies is significant if not dominant in many instances of electron-molecule interactions.

Elastic scattering of electrons has been discussed by several authors (e.g., Massey and Burhop, 1969; McDaniel, 1964; Hasted, 1964; and Christophorou, 1971). In an elastic collision the electron loses a small fraction of its kinetic energy to the target molecule. Momentum is conserved in the process and the internal energy state of the target molecule is unchanged.

If the internal energy of the target molecule is increased by way of a loss in the electron's kinetic energy we have an inelastic collision. The increase in internal energy occurs as vibrational, rotational, and/or electronic

excitation. (Ionization is not included since we have restricted the present discussion to sub-ionization electron energies.) The amount of energy lost by the electron is determined by the initial and final states of the target molecule.

Another non-elastic collision process is the so-called "superelastic" collision (Massey and Burhop, 1969). These collisions occur when the target molecule is already in an excited state when the incident electron interacts with it. The net result is an increase in the kinetic energy of the electron with a simultaneous decrease in the internal energy of the target molecule. Superelastic collisions are therefore important for thermal energy electrons and for long-lived metastable molecular states.

When a low-energy electron comes within the domain of a neutral molecule there is a possibility that the electron is attached to the molecule. A quantity known as the electron affinity (EA) is defined as the difference in energy between the neutral molecule in its ground state plus an electron at rest at infinity and the negative ion in its ground state. ("Ground state" indicates lowest electronic, vibrational, and rotational quantum states.) The EA of the molecule is thus a measure of the molecule's "ability" to retain as extra electron. A positive electron affinity would indicate that the ground state of the negative ion is at a lower energy than the ground state of the neutral molecule of the same species. If the ground state of the negative ion

is at a higher energy than the ground state of the neutral species we then have a negative EA.

In the case of a negative EA there is another quantity , which is more readily obtained from experiment, known as the vertical attachment energy (VAE) (Christophorou and Compton, 1967). This parameter is defined as the difference between the effective potential energy of the ground state of the neutral molecule and the effective potential energy of the molecular negative ion formed with the same internuclear separation of the constituent nuclei and an electron at rest at infinity. This can be written

$$VAE = U_{M^-}(R_\varepsilon^0) - U_X(R_\varepsilon^0) \qquad \text{I-1}$$

where $U_{M^-}(R_\varepsilon^0)$ is the effective potential energy of the molecular negative ion for an internuclear separation R_ε^0 and $U_X(R_\varepsilon^0)$ is the effective potential energy of the neutral molecule for the same internuclear separation. Both the EA and VAE are illustrated in Figure I-1 for negative (a) and positive (b) EA's.

Following electron attachment the unstable molecular ion may dissociate to form product atom(s) or radical(s) and ions with or without internal energy, viz.,

$$MX^{-*} \rightarrow M(\text{or } M^*) + X^- \text{ (or } X^{-*}). \qquad \text{I-2}$$

This mode of decay, referred to as dissociative attachment, is discussed in detail by Christophorou (1971).

The electron attachment process considered in the

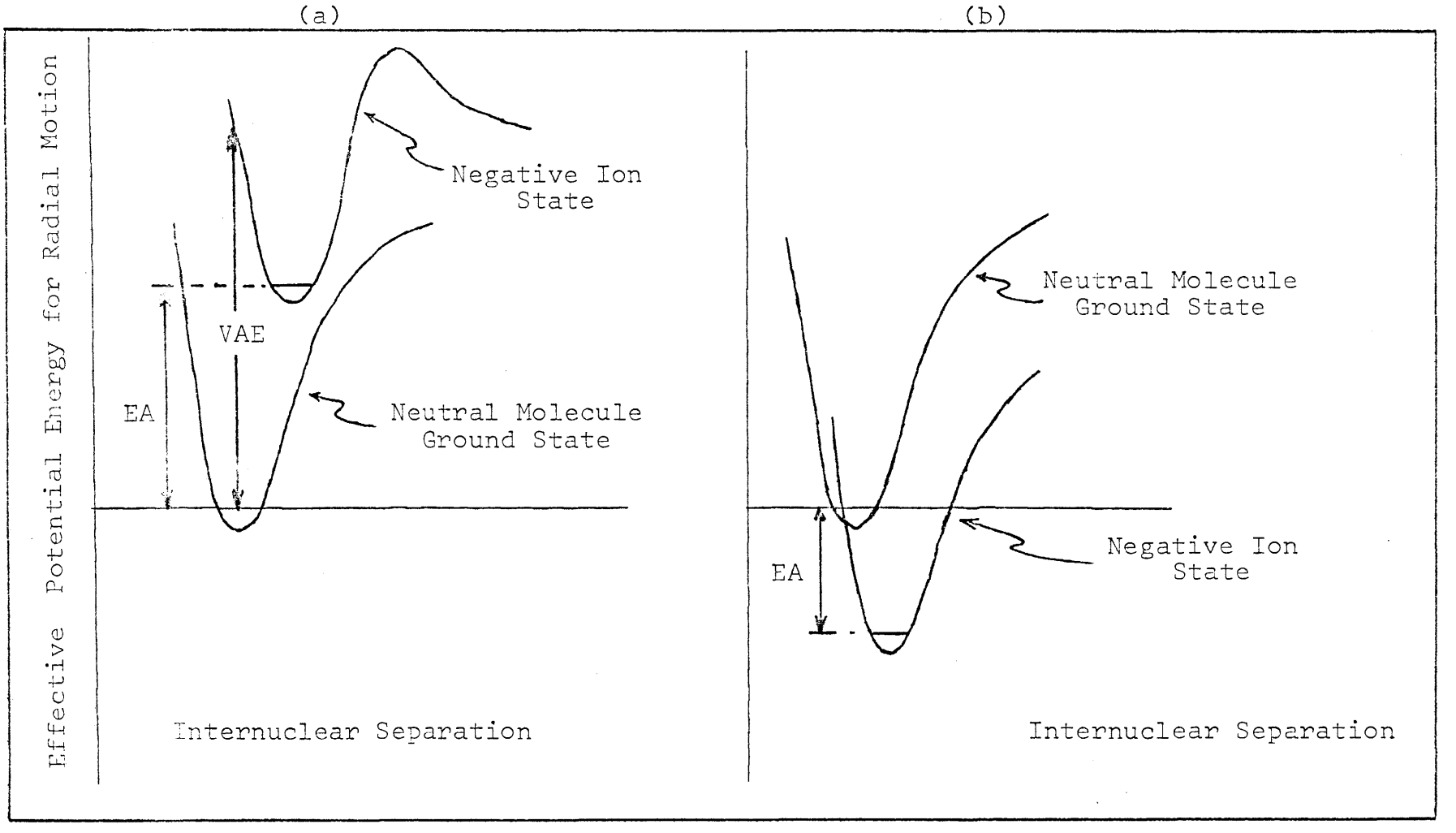

Figure I-1. Potential energy diagrams illustrating EA and VAE for diatomic molecules.

present work is transient negative ion formation followed by autodetachment of the negative ion, viz.,

$$e + MX \rightarrow MX^{-*} \rightarrow MX \text{ (or } MX^{*}) + e. \qquad \text{I-3}$$

If the resulting molecule is in a different quantum state following the collision process than it was prior to the collision then we have indirect inelastic scattering. If the final molecular state is unchanged by the collision then we have indirect elastic scattering.

The object of this work is to study negative ion resonance (NIR) states produced by the passage of an electron beam through a low pressure gas. Experimental data will be presented and discussed herein for benzene, six fluorobenzenes, and biphenyl. EA's and/or VAE's of these eight molecules will be presented along with the observed vibrational energies of the negative ions.

III. OUTLINE OF PRESENT WORK

In Chapter II the theory of electron-molecule interactions is discussed briefly with particular emphasis on negative ion resonances. Theoretical models of molecular negative ions will be elaborated upon. This is followed by a history and a description of electron beam techniques in Chapter III. A complete description of the present experimental apparatus with its operation procedures is given in Chapter IV.

Negative ion resonances in benzene are discussed in

Chapter V. Experimental results and their analysis for six fluorobenzenes and biphenyl are presented and discussed in Chapters VI and VII, respectively. Finally, a summary of the experimental results is given and certain conclusions are reached.

CHAPTER II

THEORY

I. INTRODUCTION

When a low-energy electron interacts with a neutral molecule, a compound negative ion can be formed. This "complex" is often referred to as a temporary negative ion since its lifetime is often very short (10^{-6} sec - 10^{-15} sec). Often such a negative ion formed by electron attachment is referred to as a negative ion resonance (NIR). This is an appropriate term since electron attachment to molecules occurs for a definite energy interval of the incident electron. This is evidenced as sharp structure in the interaction cross-section. (Although broad structure occurs for molecular negative ions with very short lifetimes due to the uncertainty principle.)

Although the existence of resonances due to negative ion formation is evident in the early work on electron-molecule scattering cross sections, it is only within the last fifteen years that a resonance model has been applied to electron-molecule interactions. Resonance interactions between low-energy electrons and molecules have been the subject of several recent theoretical and experimental studies. These include the work of Taylor and co-workers (1966), Bardsley and Mandl (1968), Schulz (1973), and Christophorou and co-workers (1977).

Classification of resonances according to various authors will be presented in this chapter with a brief comparison of nomenclature. Although all types of NIR's are considered, we will be primarily concerned with a particular type of NIR, namely, the single particle or shape resonance.

II. CLASSIFICATION OF NEGATIVE ION RESONANCES

In the resonance description of electron-molecule interactions, the incident electron is bound to a neutral molecule for a time which is longer than the normal transit time through the molecule. The compound system thus formed decays within 10^{-6} to 10^{-15} sec (depending upon the molecule involved) to yield a neutral molecule in either its ground state or in some excited state and an outgoing electron.

Negative ion resonances are classified according to the binding mechanism which holds the electron-molecule system together. The principal theoretical papers which have dealt with the classification of NIR's are by Taylor and co-workers (1966) and by Bardsley and Mandl (1968).

Shape Resonance

When an incident electron is trapped in the potential well associated with a molecule in its ground electronic state we have a single particle resonance (Taylor and co-workers, 1966) or shape resonance (Bardsley and Mandl, 1968). The neutral molecule exerts an attractive Coulombic force on

the incident electron in a region near the constituent nuclei. This region is surrounded by a repulsive force field (viz. a centrifugal force) produced by the electron-molecule motion. The combined forces create a potential well with a penetrable barrier, the shape of which can trap the incoming electron, hence the name shape resonance. In Figure II-1 the qualitative aspects of the potential well are shown for diatomic molecules.

A shape resonance may decay via autodetachment or via dissociative attachment.

Resonances of Excited States

Resonances associated with excited electronic states of the target molecule are referred to as core-excited resonances (Taylor, et al., 1966). The incident electron causes electronic excitation of the target molecule thereby producing a slightly positive central core. The incident electron is simultaneously bound to the excited molecule by the Coulombic attraction. Autodetachment usually occurs within a short time to yield the target molecule and a scattered electron.

Bardsley and Mandl (1968) have assigned the term Feshbach resonance to a resonance which occurs when the incident electron loses energy by exciting the target molecule and is then trapped by the excited molecule. A potential energy diagram is shown in Figure II-2 for this type of resonance. Feshbach resonances are further divided into

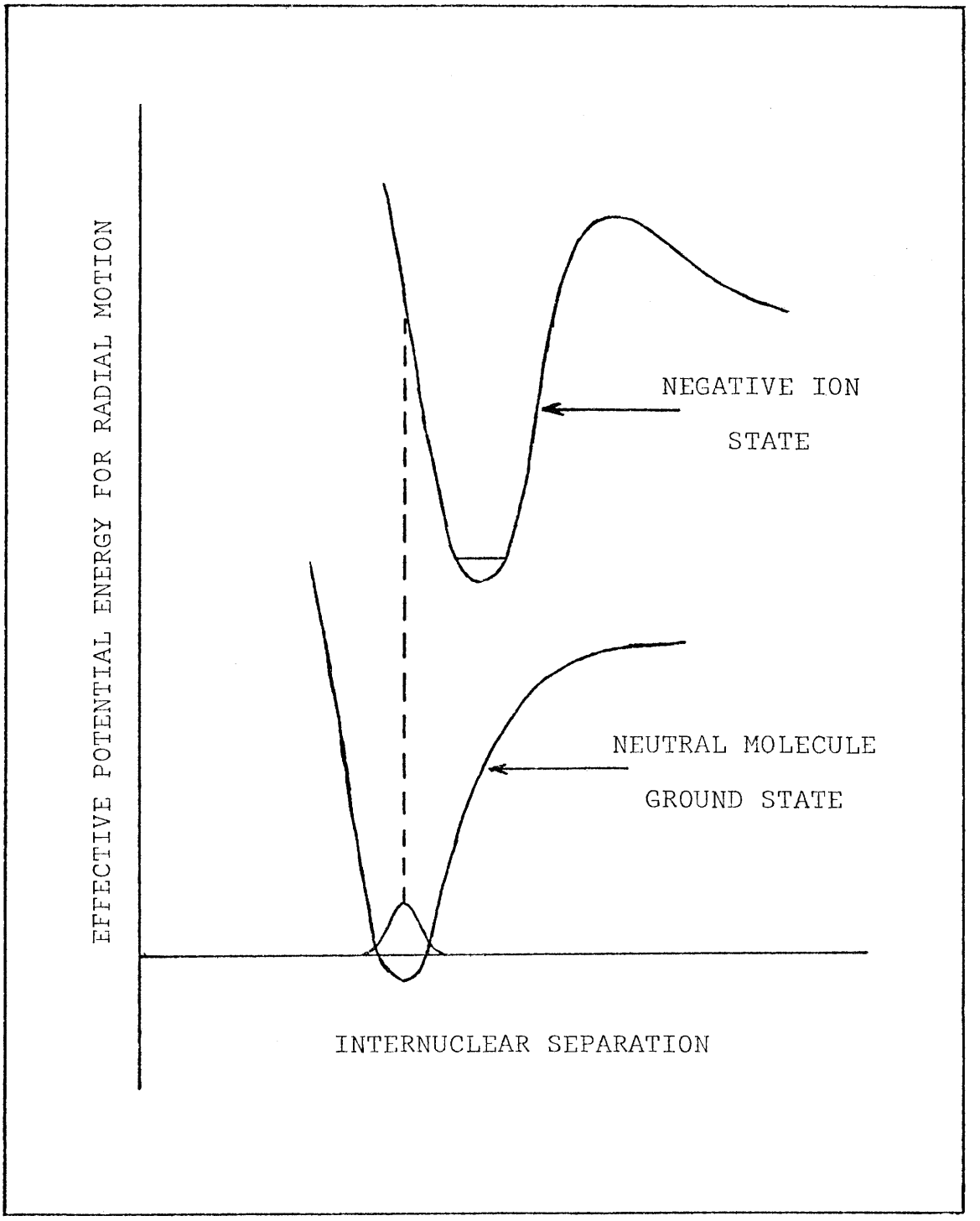

Figure II-1. Effective potential energy diagram for a shape resonance.

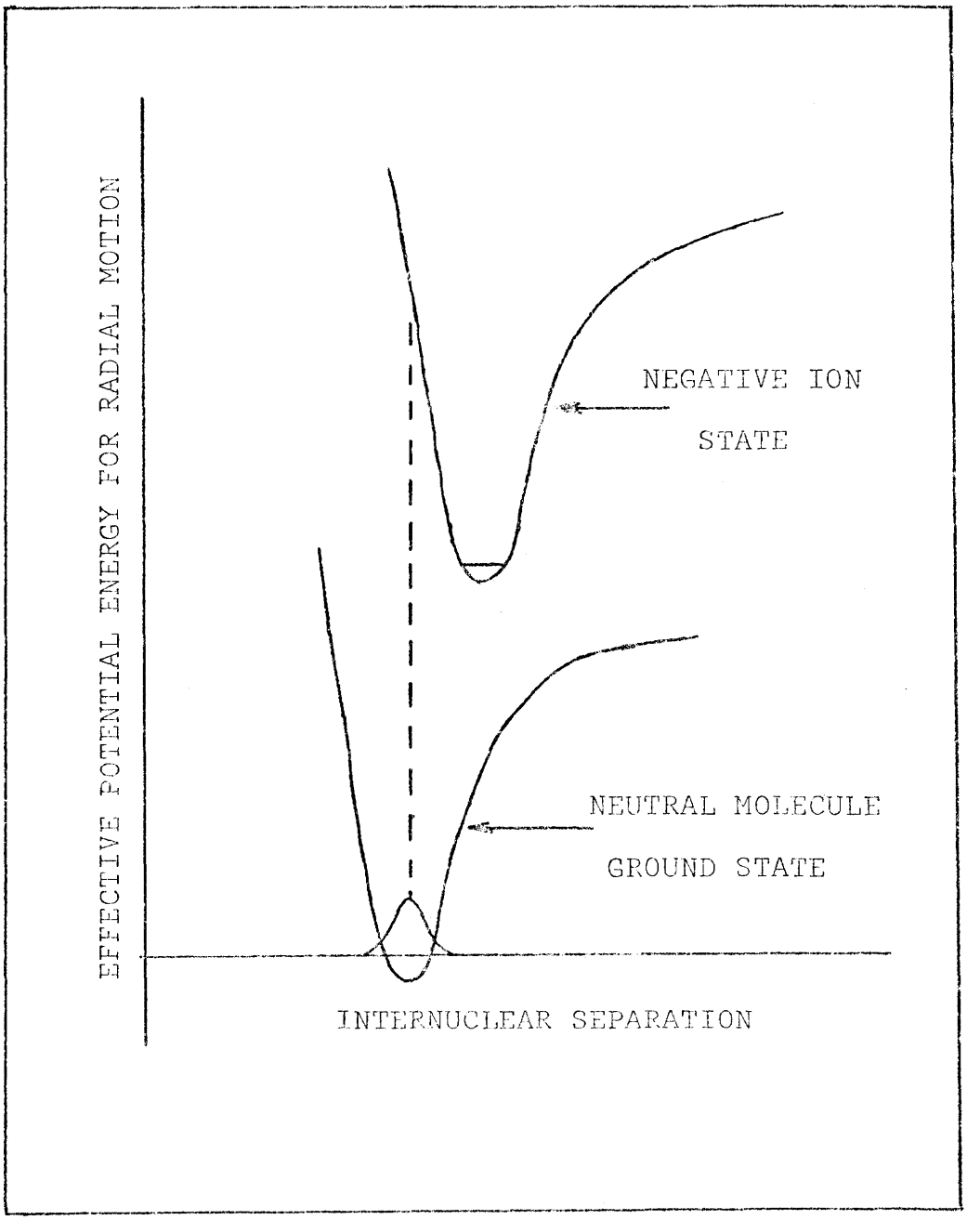

Figure II-2. Effective potential energy diagram for an electron-excited Feshbach resonance.

two types according to whether there is electronic excitation or only nuclear excitation of the target molecule. In either case the incident electron is trapped in a bound state and remains in the bound state until electronic or nuclear de-excitation of the molecule occurs, in which event the electron can attain sufficient energy to escape.

Feshbach resonances and core-excited resonances are in many cases different terms for the same type of molecular negative ion. Christophorou et al., (1977) compared the nomenclature for the various types of NIR's and gave an explanation of the physical processes involved in each type.

III. THEORETICAL APPROACHES TO NIR CALCULATIONS

There are several theoretical approaches for NIR calculations. A summary of these can be found in the review article by Nicolaides (1972). Since we are concerned only with shape resonances we can divide the theories for resonance calculations into three general areas:

1. Theories for resonances as additional "bound" states.
2. Theories for NIR's as decaying molecular states.
3. Scattering theory.

The theoretical treatment of resonances as special types of bound states solves for the expectation value of the Hamiltonian by use of an approximate trial wave function.

In the treatment of resonances as decaying states of negative molecular ions a stationary value for the complex

energy is calculated. This method proceeds according to the Kapur-Peierls theory (Herzenberg and Mandl, 1962).

Cross sections can be calculated from values for phase shifts which arise in scattering theory. These calculations treat the electron-molecule collision as a wave interaction and yield the location and positions of NIR's as well as interaction cross sections.

Electron-Molecule Resonant Scattering

Consider the Schrodinger wave equation for an electron in a short-range, spherically symmetric, spin-independent, local potential $V(\vec{r})$ centered at the origin of the coordinates, i.e.,

$$\left(-\frac{\hbar^2}{2m} \nabla^2 + V(\vec{r}) \right) \psi(\vec{r}) = \varepsilon(\vec{r})\ \psi(\vec{r}) \qquad \text{II-1}$$

where m is the electron's mass, $\hbar$ is Planck's constant divided by 2π, ε is the energy eigenvalue, and $\psi(\vec{r})$ is the state wave function. For large distances (i.e., $r \to \infty$) from the origin, the solution to the above equation is chosen as a plane wave incident in the Z - direction plus an outgoing spherically scattered wave, viz.

$$\psi(r) \underset{r\to\infty}{\sim} e^{ikz} + f(\theta)\ \frac{e^{ikr}}{r} \qquad \text{II-2}$$

where $k^2 = \frac{2mE}{\hbar^2}$

and $f(\theta)$ is the scattering amplitude.

The total cross section is related to the scattering amplitude by

$$\sigma = 2\pi \int_0^{\pi} |f(\theta)|^2 \sin\theta \, d\theta. \qquad \text{II-3}$$

The solution of equation II-1 which satisfies equation II-2 would yield the total cross section as given by equation II-3.

A partial wave expansion is used to solve equation II-1 with the restriction that equation II-2 is also satisfied. We assume a solution to equation II-1 to be

$$\psi(\vec{r}) = \frac{1}{r} \sum_{\ell=0}^{\infty} A_\ell(k^2)\, u_\ell(\vec{r})\, P_\ell(\cos\theta) \qquad \text{II-4}$$

where $P_\ell(\cos\theta)$ are the Legendre polynomials, the coefficients $A_\ell(k^2)$ are determined by equation II-2, and $u_\ell(\vec{r})$ is the radial wave function.

Substituting equation II-4 into equation II-1 we obtain (making use of the orthogonality of the Legendre polynomials)

$$\left(\frac{d^2}{dr^2} - \frac{\ell(\ell+1)}{r^2} - U(r) + k^2 \right) u_\ell(r) = 0 \qquad \text{II-5}$$

where $U(r) = 2mV(r)\hbar^{-2}$.

If we restrict ourselves to a short range potential we have (see Burke, 1977)

$$u_\ell(r) \underset{r\to\infty}{\sim} \sin(kr - \tfrac{1}{2}\ell\pi + \delta_\ell) \qquad \text{II-6}$$

which defines the relationship between the real phase shift, δ_ℓ , and the radial wave function $u_\ell(r)$.

In order for equation II-2 and equation II-4 to have the same asymptotic limit the coefficients $A_\ell(k^2)$ must be properly chosen. We expand e^{ikz} in a polynomial expansion,

viz.

$$e^{ikz} = \sum_{\ell=0}^{\infty} (2\ell+1)\, i^{\ell} j_{\ell}(kr)\, P_{\ell}(\cos\theta) \quad . \qquad \text{II-7}$$

This yields the necessary values of the coefficients $A_{\ell}(k^2)$ in equation II-4, viz.

$$A_{\ell}(k^2) = \frac{1}{k}(2\ell+1)\, i^{\ell} e^{i\delta_{\ell}} \quad . \qquad \text{II-8}$$

Combining equation II-8, II-4, and II-6 we have

$$f(\theta) = \frac{1}{2ik} \sum_{\ell=0}^{\infty} (2\ell+1)\, (e^{2i\delta_{\ell}} - 1)\, P_{\ell}(\cos\theta) \quad . \qquad \text{II-9}$$

This value of the scattering amplitude in equation II-3 yields

$$\sigma = \frac{4\pi}{k^2} \sum_{\ell=0}^{\infty} (2\ell+1)\, \sin^2 \delta_{\ell} \qquad \text{II-10}$$

or

$$\sigma = \sum_{\ell=0}^{\infty} \sigma_{\ell} \qquad \text{II-11}$$

where we have defined σ_{ℓ} as the ℓ th partial wave cross section.

The difficulty in this theoretical treatment is how to find the appropriate values for the partial wave phase shifts. Burke (1977) has determined that, for real k, the total phase shift δ_{ℓ} has a "background" component $\delta_{o_{\ell}}$ and a "resonance" component $\delta_{R_{\ell}}$, and that

$$\delta_{\ell}(k) = \delta_{o_{\ell}}(k) + \delta_{R_{\ell}}(k) \quad . \qquad \text{II-12}$$

He further states that for shape resonances

$$\delta_{R_{\ell}}(k) = \tan^{-1} \frac{\frac{1}{2}\Gamma_{\ell}}{\varepsilon_{R_{\ell}} - \varepsilon} \qquad \text{II-13}$$

where Γ_{ℓ} is the resonance width at half maximum and $\varepsilon_{R_{\ell}}$ is

the resonance energy. Using the values given in equations II-12 and II-13 in equation II-10 we have

$$\sigma = \frac{4\pi}{k^2} \sum_{\ell=0}^{\infty} (2\ell+1) \sin^2\left(\delta_{o\ell} + \tan^{-1} \frac{\frac{1}{2}\Gamma_\ell}{\varepsilon_{R\ell} - \varepsilon} \right) . \qquad \text{II-14}$$

The ℓ th partial wave cross section is thus

$$\sigma_\ell = \frac{4\pi}{k^2} (2\ell+1) \sin^2\left(\delta_{o\ell} + \tan^{-1} \frac{\frac{1}{2}\Gamma_\ell}{\varepsilon_{R\ell} - \varepsilon} \right) . \qquad \text{II-15}$$

Using the preceding equation we can generate semi-empirical values for the ℓ th resonance cross section, as a function of electron energy, for known (experimentally determined) values of Γ_ℓ, $\delta_{o\ell}$, and $\varepsilon_{R\ell}$. This will be done in Chapter V for the 4.80 eV benzene NIR.

IV. SUMMARY

In the qualitative description of a shape resonance, the trapping potential well occurs only for nonzero angular momentum states (i.e. $\ell \geq 1$). We can think of the additional orbital occupied by the extra electron as being a bound orbital for only a short time.

As ℓ increases the well depth decreases and the barrier becomes narrower until the limiting value of ℓ is reached. In that event the potential as seen by the electron is completely repulsive.

This qualitative description agrees well with the partial wave scattering theory we have outlined; whereby only p - wave (ℓ = 1) or higher wave scattering occurs for shape resonances.

CHAPTER III

ELECTRON BEAM TECHNIQUES FOR THE STUDY OF NEGATIVE ION RESONANCES

I. INTRODUCTION

Electron beam techniques have been used for several years to study negative ion resonances. Several combinations of experimental techniques are used for the study of NIR's, with each combination yielding a different property of the electron-molecule resonant interaction. Figure III-1 illustrates the basic components of electron beam experiments.

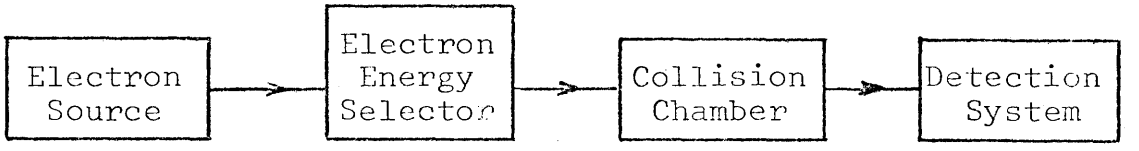

Figure III-1. Components of electron beam experiments.

In this chapter a brief comparison of electron beam techniques is presented, with emphasis on the electron transmission method. A more complete description of electron beam techniques can be found in recent literature (e.g. Kuyatt, 1968; Massey and Burhop, 1969; and Schulz, 1973).

II. ELECTRON ENERGY SELECTORS

In any electron beam experiment a source of electrons is required. The most common source of electrons is a directly or an indirectly heated filament. It is usually

desirable that this source of electrons has constant emissivity and be reasonably unaffected by the gas under study. Various metals have been used as filaments, including tungsten and iridium. One of the most desirable filaments which satisfies the above mentioned criteria is the thoriated iridium filament.

Once a source of electrons has been found, the next step is to produce an electron beam with a very narrow energy spread, i.e. an approximately monenergetic beam. This component of all beam experiments is a necessity since most of the phenomena of interest occur within a narrow energy range. As an example, the vibrational levels of a shape resonance of a large molecule (e.g. C_6F_6) are separated by $\lesssim$ 0.06 eV. Therefore, the electron energy spread should be much narrower than 0.06 eV in order to observe such structure.

Production of a quasi-monoenergetic beam of electrons is achieved by the use of an electron energy selector (often called electron monochromator). This device produces a dispersion in energy of the electron beam by a combination of electric and/or magnetic fields. The full width at half maximum (FWHM) of the electron energy distribution thereby produced can be less than 0.02 eV with a current of $\sim 5. \times 10^{-9}$ A.

The geometry or configuration of the dispersing fields are divided into two basic categories; those operating in the absence of magnetic fields and those with an axial magnetic field. Energy selectors which operate in magnetically

field-free regions are preferred by many investigators since external magnetic effects are eliminated (Golden, 1973). Examples of such energy selectors are the 180° concentric spherical "monochromator" (Meyer and co-workers, 1965 and Simpson, 1964), the 127° coaxial cylindrical "monochromator" (Hughes and Rojansky, 1929 and Marmet and Kerwin, 1960), and the parallel plate selector (Simpson, 1961). The reader is referred to the above mentioned articles for details of operation and performance of these analyzers.

When studying low-energy electron-molecule interactions it is often desirable to have an axial magnetic field which prevents spreading of the electron beam and allows for negative ion and electron separation. Golden (1973) discussed the undesirable effects of a magnetic field in the interaction region. Nevertheless, confining magnetic fields often are used as part of electron beam devices having high precision and sensitivity.

Fox and co-workers (1955) developed the retarding potential difference (RPD) method to reduce the spread in the electron beam energy. In this method, electrons are retarded at one electrode of the electron gun to create a sharp low-energy cutoff of the energy distribution. This cutoff potential is modulated by a small voltage with only the difference in current being detected. Only a portion of the energy distribution of the electrons from the gun is used. Electron energy spreads of 0.1 eV (FWHM) can be obtained with this method. One of the main difficulties associated with

this method is the ensuing noise on the difference signal.

Another energy selector designed for use with an axial magnetic field in electron beam studies is the trochoidal electron "monochromator." The design and operation of this device is described in detail in Chapter IV. Briefly, electrons are thermally emitted from a hot filament and accelerated along an axial magnetic field ($\vec{B}$). They are then decelerated as they pass into a region of crossed uniform electric field ($\vec{E}$) produced by parallel plates. Dispersion of the electron beam occurs in this region by means of a deflection of the beam along an axis perpendicular to both $\vec{E}$ and $\vec{B}$. Dispersion proceeds according to the axial velocities of the electrons with only the electrons reaching an exit aperture being transmitted into the collision chamber. Electron energy distributions of $\lesssim$0.02 eV (FWHM) can be obtained with this "monochromator." Difficulties arise from optical focusing of the beam as the accelerating voltage is increased (see Chapter IV). These can be minimized by improved mechanical design of aperture dimensions. A comparison of electron beam properties is presented in Table III-1 for electron "monochromators" used for low-energy electron beam experiments.

III. METHODS OF DETECTION OF NIR'S

To study molecular negative ion resonances we must have a region for electron-molecule interactions to occur. This can be merely a cell containing a fixed quantity of gas

TABLE III-1

COMPARISON OF ELECTRON BEAM-PROPERTIES FOR DIFFERENT "MONOCHROMATORS"

Instrument Design	Optimum values FWHM (eV)	Current[§] ($\times 10^{-9}$A)	Reference
Without B Fields			
180° Sperical	0.07 0.02-0.06	100	Kuyatt and Simpson (1967) Schulz (1973)
127° Coaxial Cylinders	0.06-0.08 0.02-0.06	100	Kuyatt and Simpson (1967) Schulz (1973)
With Axial Magnetic Field			
Retarding Potential Difference*	0.1	10	Christophorou (1971)
Trochoidal Electron "Monochromator"	0.03-0.04 0.02	5 5	Sanche and Schulz (1972) Present Work

*Although the Retarding Potential Difference device is not a true "monochromator," the method is included here for comparison.

[§]These properties of electron beams depend strongly on experimental paramenters the discussion of which is beyond the scope of the present work. They are presented here as a brief comparison between optimum values.

through which the quasi-monoenergetic beam of electrons is passed (transmitted). It might be a dynamic system with gas flowing through the cell while a constant pressure is maintained inside the volume of the collision chamber. Another electron-molecule interaction technique is the crossed beam method. In this method a molecular beam is produced which then intercepts the electron beam at right angles. This greatly reduces the Doppler spreading of the relative energies of the molecules in the electron-molecule interaction.

Regardless of which of the above two methods is used, a detection system completes the essential components of an electron spectrometer. The detector type is determined by the property of the electron-molecule resonance interaction under study. For elastic, vibrational, and electronic excitation cross section measurements, an electron energy loss analyzer is used. With this detector the energy dependence of the elastic or inelastic cross sections (at a particular angle with respect to the incident beam direction) is found. By fixing the incident electron energy and varying the detector position with respect to the incident beam direction the angular distribution of the scattered electrons can be measured.

Likewise, the total metastable cross section and optical excitation cross section are obtained when using a metastable detector and a photon detector, respectively. The

difficulties encountered with these methods are discussed by several authors (Christophorou, 1971; Bates, 1962; Hasted, 1964).

For the past 20 years, inelastic cross sections have been measured with the trapped electron method. This method has been used by many research groups (e.g., Schulz, 1958; Compton, Christophorou and Huebner, 1966; Pisanias, et al., 1972). In this method an electron beam is passed through a gas and all (in 4π geometry) of the inelastically scattered electrons are collected. Trapping of these inelastically scattered electrons is accomplished by either of two techniques, a "zero energy" electron scavenger, or an electrostatic potential well.

The electron scavenger technique is described in detail by Christophorou (1971). In this method a "scavenger" gas, such as SF_6, having a very sharp and intense electron attachment cross section at $\sim$0.0 eV is admitted to the collision chamber containing the sample gas. Electrons of near zero energy which are inelastically scattered from the sample gas are attached to the scavenger gas molecules forming negative ions. These are detected with a mass spectrometer. The negative ion current is plotted versus the incident electron energy. This plot provides the so-called threshold electron excitation sprectrum of the compound under study.

Another way to trap the inelastically scattered electrons is to use an electrostatic potential well defined

by component electrodes in the collision chamber. A typical schematic of such a device is shown in Figure III-2.

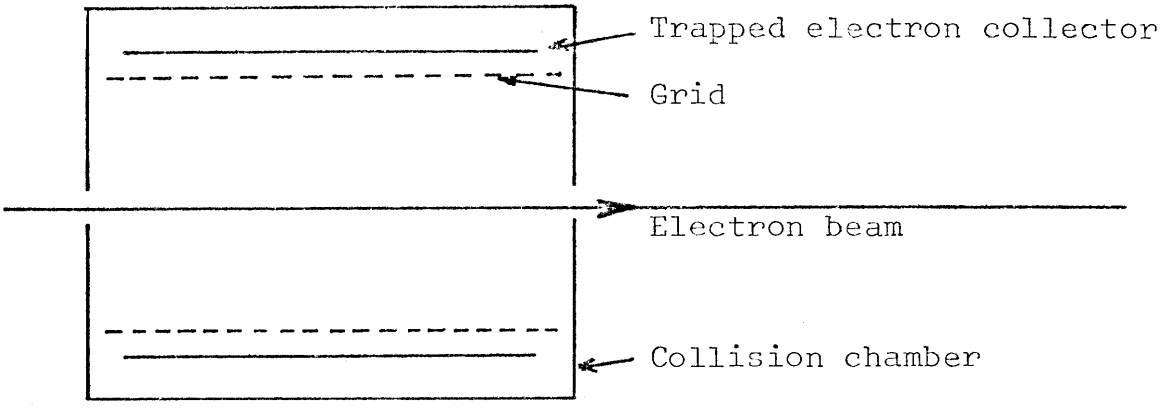

Figure III-2. Schematic diagram of a trapped electron collector which produces an electrostatic potential well.

An electrostatic potential is applied to the trapped electron collector in such a manner that it is positive with respect to the grid and collision chamber. The penetration of this potential through the grid produces a potential well between the axis of the beam and the collision chamber electrodes. Electrons which have been inelastically scattered by the sample gas and, in the process, have lost essentially all of their kinetic energy to the sample gas molecules cannot escape from this potential well and are thus collected. (The kinetic energy of the electron should be less than the trap depth in order to be trapped.) The collected current is plotted as a function of the incident electron energy.

The most common method of negative ion resonance detection and analysis in use at this time is the electron

transmission method. The basis of measurement in this method is the attenuation of a monoenergetic electron beam during its passage through a sample gas. The electron energy is varied in the collision chamber while the unscattered (transmitted) current is measured as a function of the incident electron energy. Structure in the total scattering cross section is obtained from the values of the transmitted current as it varies with electron energy. Resonances are located and assigned from structure in the total scattering cross section.

Electron transmission spectroscopy has been employed since 1963 (Simpson and Fano, 1963) to locate resonances due to temporary negative ion formation. This method is highly sensitive for negative ion resonance detection. However, since no angular distribution measurements can be made with this method, assignment of resonance configurations is difficult and other methods must be employed. Also, electron transmission spectroscopy does not easily provide information as to the final states of the molecules following decay of the resonance. Neither does it provide information as to the magnitude of the total scattering cross section. Though lacking in versatility, electron transmission studies are the most sensitive for the location of NIR's in atoms and molecules.

CHAPTER IV

EXPERIMENTAL APPARATUS AND PROCEDURE

I. INTRODUCTION

One of the experimental methods used to locate negative ion resonances is electron transmission spectroscopy. In this method a quasi-monenergetic beam of electrons is generated, passed through a low-pressure (10^{-3} to 10^{-5} torr) gas, and subsequently, into a current collector where only the unscattered beam is collected.

Electron transmission experiments were first performed by Simpson and Fano (1963). This work was soon followed by Schulz (1964) and Kuyatt, et al. (1964) and led to the more recent techniques employed by Mathur and Hasted (1976), Burrow and co-workers (1976), and VanVeen and Plantenga (1976 a,b,c).

In the present work, electron transmission experiments are performed using a trochoidal electron monochromator as the electron beam source and a derivative technique for signal enhancement. The electron gun, monochromator, collision chamber, and detection apparatus are described in detail in this chapter. Energy calibration methods and operation procedures are also discussed.

II. HISTORY OF THE TROCHOIDAL ELECTRON MONOCHROMATOR

An axial magnetic field is often employed in electron

beam experiments to collimate the electron beam. With this in mind, an electron energy selector was designed by Stamatovic and Schulz (1968) to make use of the axial magnetic field as the energy dispersion mechanism. This was accomplished by passing the beam through an electric field region which is at right angles to the magnetic field. Since the resulting electron path in this region is a trochoid, the energy selector is called a trochoidal electron monochromator (TEM).

The basic design of the TEM has been developed by Sanche and Schulz (1971) for electron transmission spectroscopy of atoms (Sanche and Schulz, 1972 a,b), diatomic molecules (Sanche and Schulz, 1971), triatomic molecules and certain hydrocarbons (Sanche and Schulz, 1973). Additional studies by Nenner and Schulz (1975) have shown the capability of the TEM to locate negative ion resonances and therefore to yield EA's and/or VAE's for even larger molecules.

Groups other than those at the Mason Laboratory of Yale University who have used the TEM design are:

1. D. Spence at Argonne National Laboratory for studies of atomic oxygen (Spence and Chupka, 1974), helium (Spence, 1975 b), and molecular halogens (Spence, 1974);
2. D. F. Dance and I. C. Walker at the University of Stirling, Stirling, Scotland, in their investigations of threshold energy-loss spectra for several molecules (Dance and Walker, 1973);

3. M. V. Kurepa and co-workers at the Institute of Physics, Belgrad, Yugoslavia, for measurements of electron-atom (Kurepa, et al., 1974) and electron-molecule (Kurepa, et al., 1976) interactions;
4. R. Abouaf and co-workers (1976) at the Laboratorie de Collisions Electroniques, Universite' Paris-Sud, Orsay, France, to study dissociative attachment in NO_2 and CO_2 by electron impact;
5. E. H. VanVeen and F. L. Plantenga (1975, 1976 a,b,c) at the University of Leyden, The Netherlands, studied electronic excitation spectra of several large molecular species; and
6. E. P. Fesenko and L. V. Iogansen (1977) with their studies of benzene at the All-Union Textile and Light Industry Correspondent Institute in Moscow, U. S. S. R.

We realized that the TEM design has been found useful for producing a collimated, quasi-monoenergetic electron beam. For this reason we have used this design in the present experiment.

III. DESCRIPTION OF EXPERIMENTAL APPARATUS

Electron Gun

The source of electrons is a directly heated, thoriated iridium filament obtained from Electron Technology, Kearney, New Jersey. This type of filament was chosen because of its high emissivity (Hanley, 1948) and resistance to poisoning

by reactive environments (Holloway, 1972). The filament is a ribbon 0.05 mm thick and 0.68 mm wide with an active length of 5.0 mm. The mounting arrangement is shown in Figure IV-1. Component (F) is the thoriated iridium filament.

The first electrode (1) (Figure IV-1) is maintained at a potential which is positive ($\sim$ + 5.0 volts) with respect to the center filament to provide efficient extraction of electrons. The dimensions of (1) as well as those of (2), (3), (4), (5), and (R) are shown in Figure IV-2 with aperture dimensions given in Table IV-1.

Electrons passing through a three element electrostatic lens (1), (2), and (3) are focused into the energy selection region. The energy spread of the beam thereby produced is typically six-tenths of an electron volt (full-width at half maximum).

The filament power supply is a Lambda Regulated Power Supply (Model LH 119 FM). Typical filament heating currents are from 3.8A to 4.3A.

Trochoidal Electron Monochromator (TEM)

Upon exiting aperture (3) the electron beam enters a region of crossed electric field provided by two solid semi-cylinders or dees (8) where parallel faces are separated by 1.57 mm. Since the entire apparatus is in an aligning magnetic field there is a force on the electrons which is perpendicular to both the magnetic field $\vec{B}$ and the electric field $\vec{E}$. This provides the mechanism for energy selection

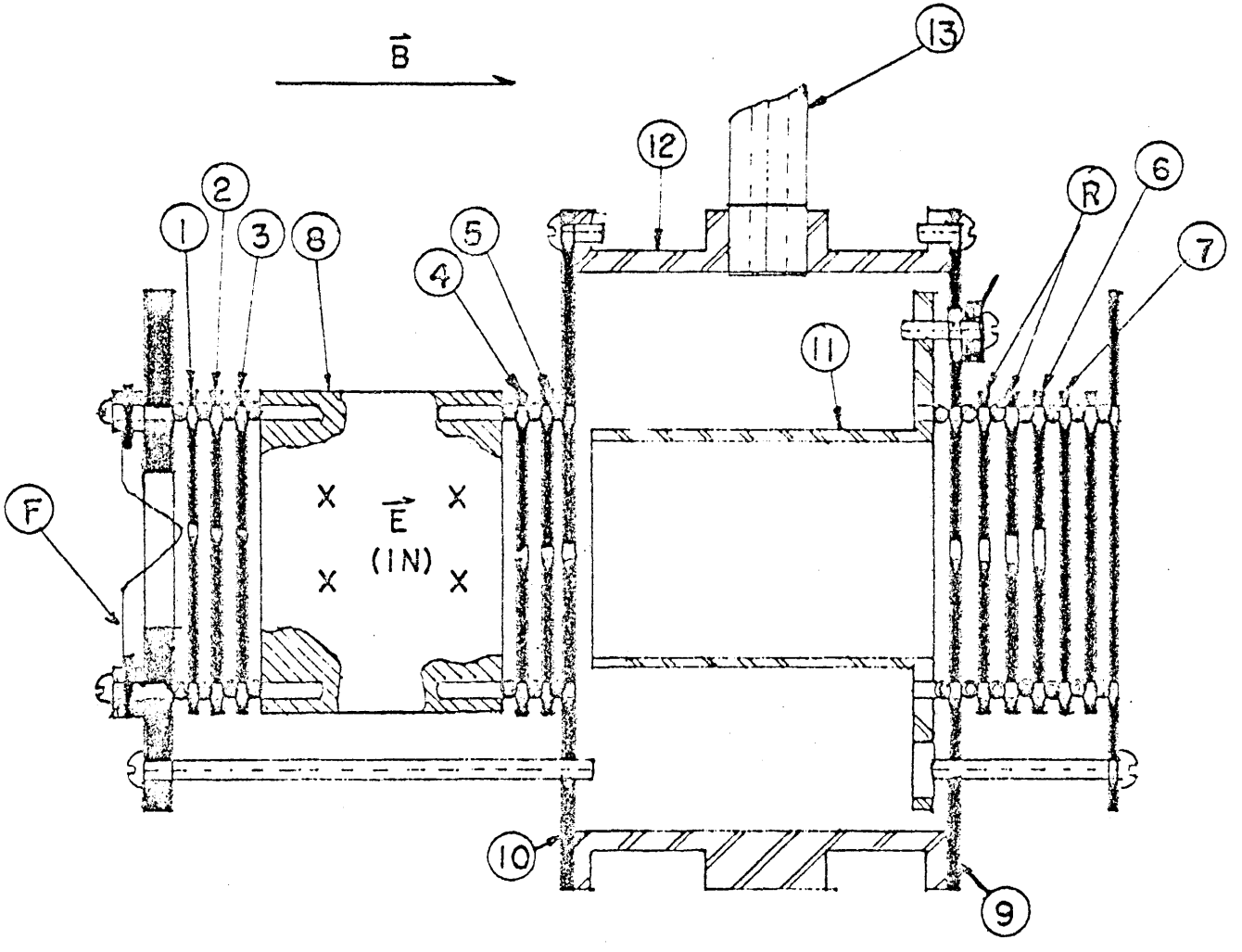

Figure IV-1. Schematic diagram of the electron transmission apparatus.

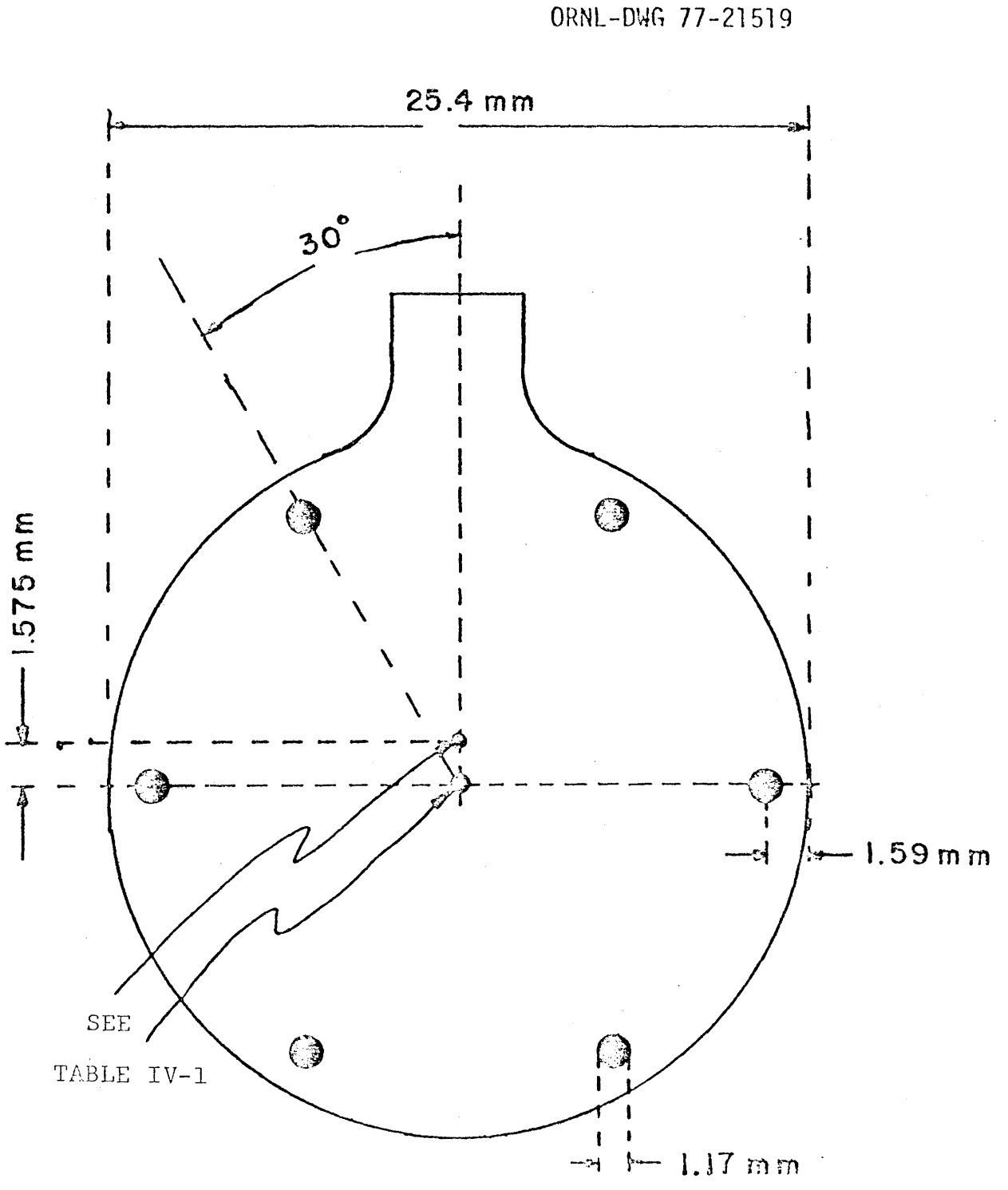

Figure IV-2. Illustration of an individual electrode.

TABLE IV-1

APERTURE DIMENSIONS OF ELECTRODES OF THE TROCHOIDAL ELECTRON MONOCHROMATOR

	Electrode	Aperture Diameter	Aperture Position
(1)	Extraction Electrode	1.00 mm	1.575 mm off center
(2)	Electrostatic Lens Element	0.50 mm	1.575 mm off center
(3)	Electrostatic Lens Element	0.25 mm	1.575 mm off center
(4)	Electrostatic Lens Element	0.50 mm	Center
(5)	Electrostatic Lens Element	0.50 mm	Center
(R)	Retarding Electrode	1.30 mm	Center
(R)	Retarding Electrode	1.60 mm	Center
(6)	Shield	1.80 mm	Center
(7)	Collector	No aperture	----------
(9)	Collision Chamber Exit	1.00 mm	Center
(10)	Collision Chamber Entrance	0.75 mm	Center

since only electrons of appropriate energy pass through the center aperture in (4) and subsequently into the collision chamber.

Crossed electric and magnetic fields have long been used in mass spectroscopic studies (Bleakney and Hipple, 1938). Bailey (1960) made use of the same principle for ion separation and analysis. In 1966, Barr and Perkins (1966) developed an electron energy analyzer using an $\vec{E} \times \vec{B}$ geometry.

If $\vec{B}$ is the aligning magnetic field and $\vec{E}$ is the orthogonal electric field, there will be a deflection of the electron's path in a direction perpendicular to both $\vec{B}$ and $\vec{E}$. These vectors are as shown in Figure IV-3.

In general, the deflection velocity is $\vec{v}_d = \frac{\vec{E} \times \vec{B}}{B^2}$, since $\vec{E} \perp \vec{B}$ we have

$$\vec{v}_d = \frac{E}{B} \hat{e}_x \qquad \text{IV-1}$$

The time in the dee region, t, is given by

$$t = \frac{L}{v_{oz}} \quad \text{where} \qquad \text{IV-2}$$

L is the length of the dees,
v_{oz} is the initial speed in the z-direction $= \left(\frac{2\varepsilon}{m}\right)^{\frac{1}{2}}$
ε is the energy of the electron upon entering the dee region, and m is the mass of the electron.

The time, t, is also given by

$$t = \frac{D}{v_d} \quad \text{, where} \qquad \text{IV-3}$$

D is the deflection distance along $\hat{e}_x$ and
v_d is the drift speed along $\hat{e}_x$ given by equation IV-1

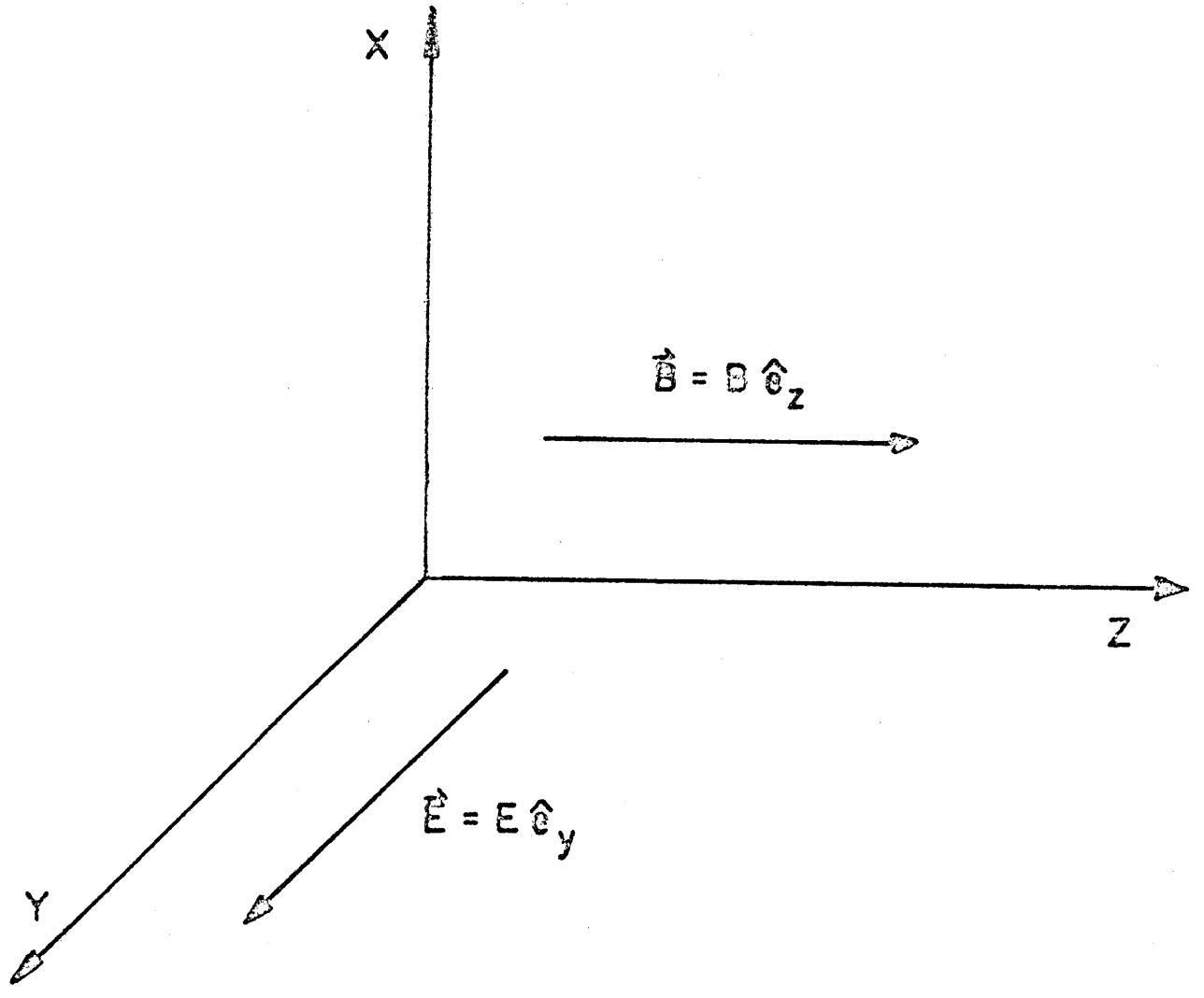

Figure IV-3. Coordinate diagram showing the electric field and magnetic field directions.

Treating the dee region as a parallel plate capacitor we have, to first order (ignoring fringing effects), the electric field, E, in the dee region given by,

$$E = \frac{V}{d} \text{ , where} \qquad \text{IV-4}$$

V is the deflection voltage and
d is the separation of the dees.

Solving equations IV-1 through IV-4, we have

$$D = \frac{LV}{Bd} \varepsilon^{-\frac{1}{2}} \left(\frac{m}{2}\right)^{\frac{1}{2}} \qquad \text{IV-5}$$

The deflection, D, is therefore inversely proportional to B and directly proportional to V. In addition, the deflection varies as $\varepsilon^{-\frac{1}{2}}$.

The energy spread of the generated electron beam is primarily due to the finite dimensions of the apertures in (3) and (4) (see Figure IV-1) and the defection distance, D. This is clearly illustrated in Figure IV-4. Electrons with energy $\varepsilon+\frac{1}{2}\Delta\varepsilon$ would undergo a deflection $D-\frac{1}{2}(S_1+S_2)$ while electrons of energy $\varepsilon-\frac{1}{2}\Delta\varepsilon$ would undergo a deflection $D+\frac{1}{2}(S_1+S_2)$.

The fractional energy spread, to first order, is

$$\frac{\Delta\varepsilon}{\varepsilon} = \frac{2(S_1+S_2)}{D} \qquad \text{(Stamatovic and Schulz, 1970)}$$

where S_1 is the aperture diameter in (3),
S_2 is the aperture diameter in (4) and
D is the deflection distance. (see Figure IV-4)

Roy (1972) attempted to calculate the energy spread of the beam to higher order to determine optimum design parameters. Large discrepancies are observed between Roy's calculations and the present experimental results. We feel that this is due primarily to spiraling of the beam as described by

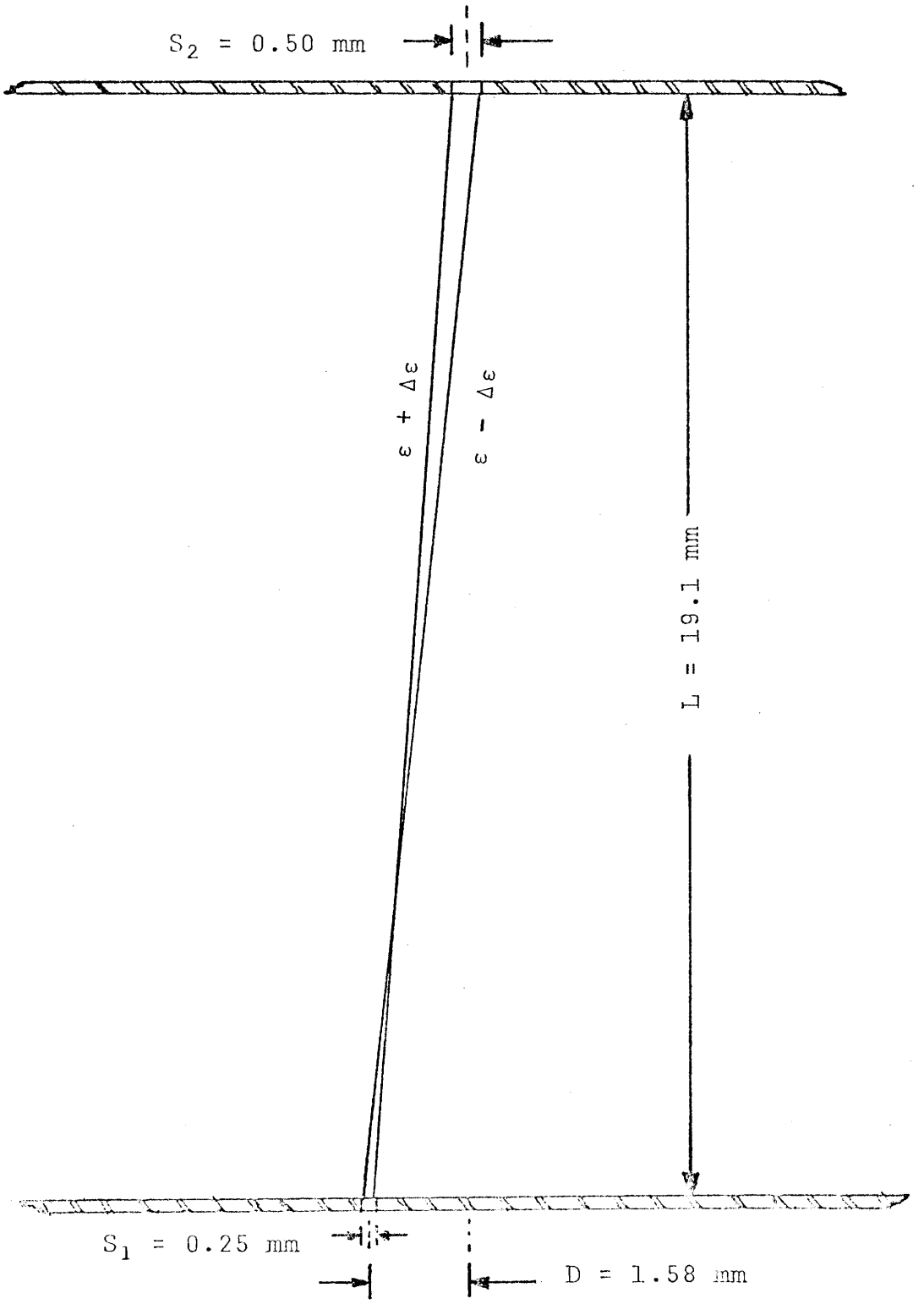

Figure IV-4. Diagram illustrating extreme paths of electrons in the deflection region.

Taylor, et al. (1974) for which Roy failed to consider.

We have measured the FWHM of our electron beam exiting the TEM and have found it to be ~0.017 eV with a current of $\sim 10^{-9}$A.

Collision Chamber

The electron beam exiting the TEM is then accelerated, between (5) and (10), into the interaction region. This is shown in Figure IV-1. The dimensions of the collision chamber are shown in Figure IV-5.

The sample gas enters the collision chamber through a ¼" diameter copper tube (13) (Figure IV-1) through a gas manifold. The gas then flows from the collision chamber through two ¼" openings in the collision chamber into the main vacuum chamber. We thus operate with dynamic gas flow conditions.

Inside the collision chamber is a coaxial cylinder which is electrically insulated from the collision chamber. The dimensions of this cylinder are shown in Figure IV-6. By applying a small sinusoidal voltage to this cylinder we modulate the electron's energy in the collision chamber. Although this causes an additional broadening of the beam energy distribution, the level of the modulation is kept small (10mV to 50mV) so as to minimize this effect.

Current Collector

The transmitted electron is collected by a Faraday cup (6) and (7) of Figure IV-1 which follows two retarding

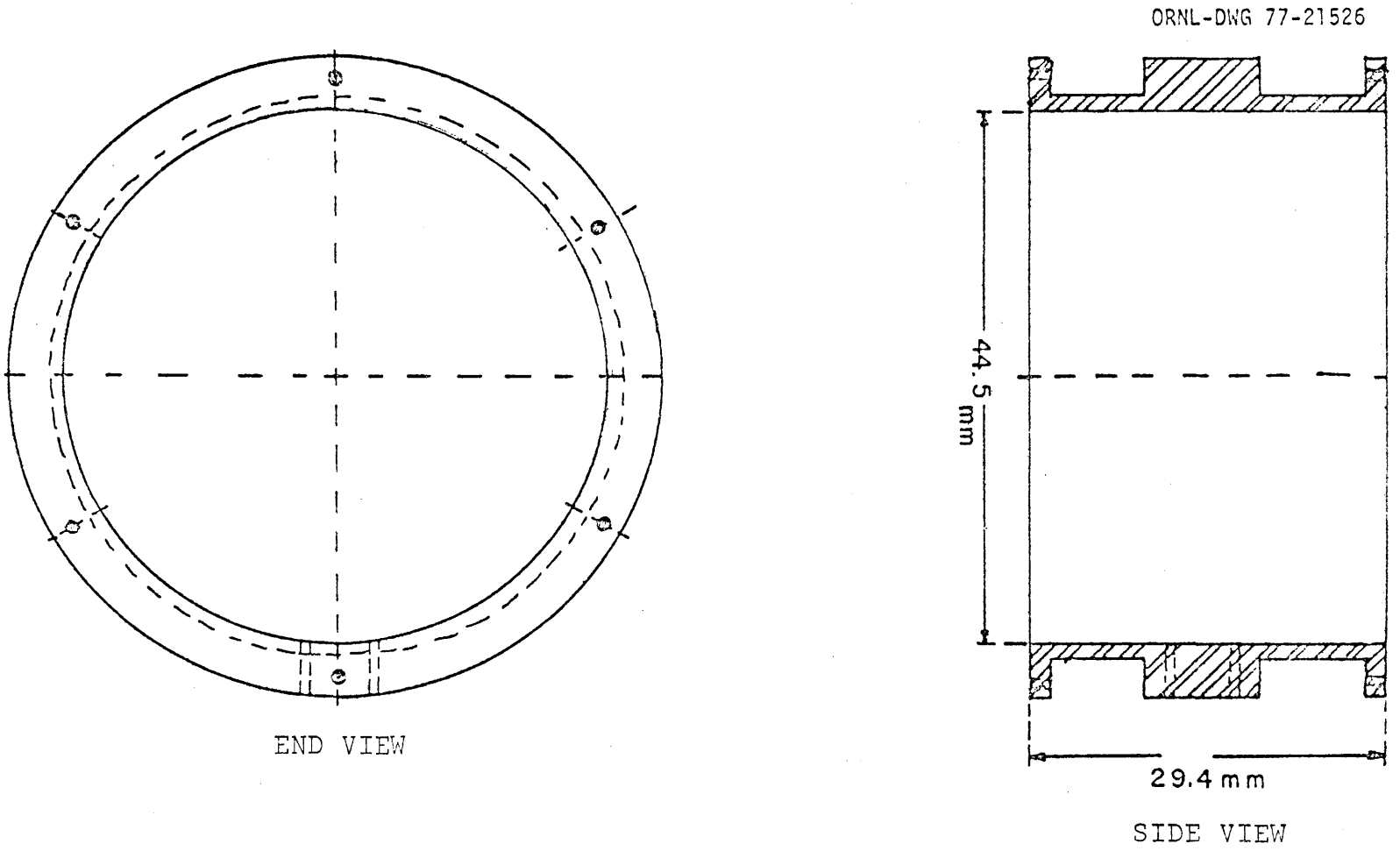

Figure IV-5. Schematic diagram of the collision chamber.

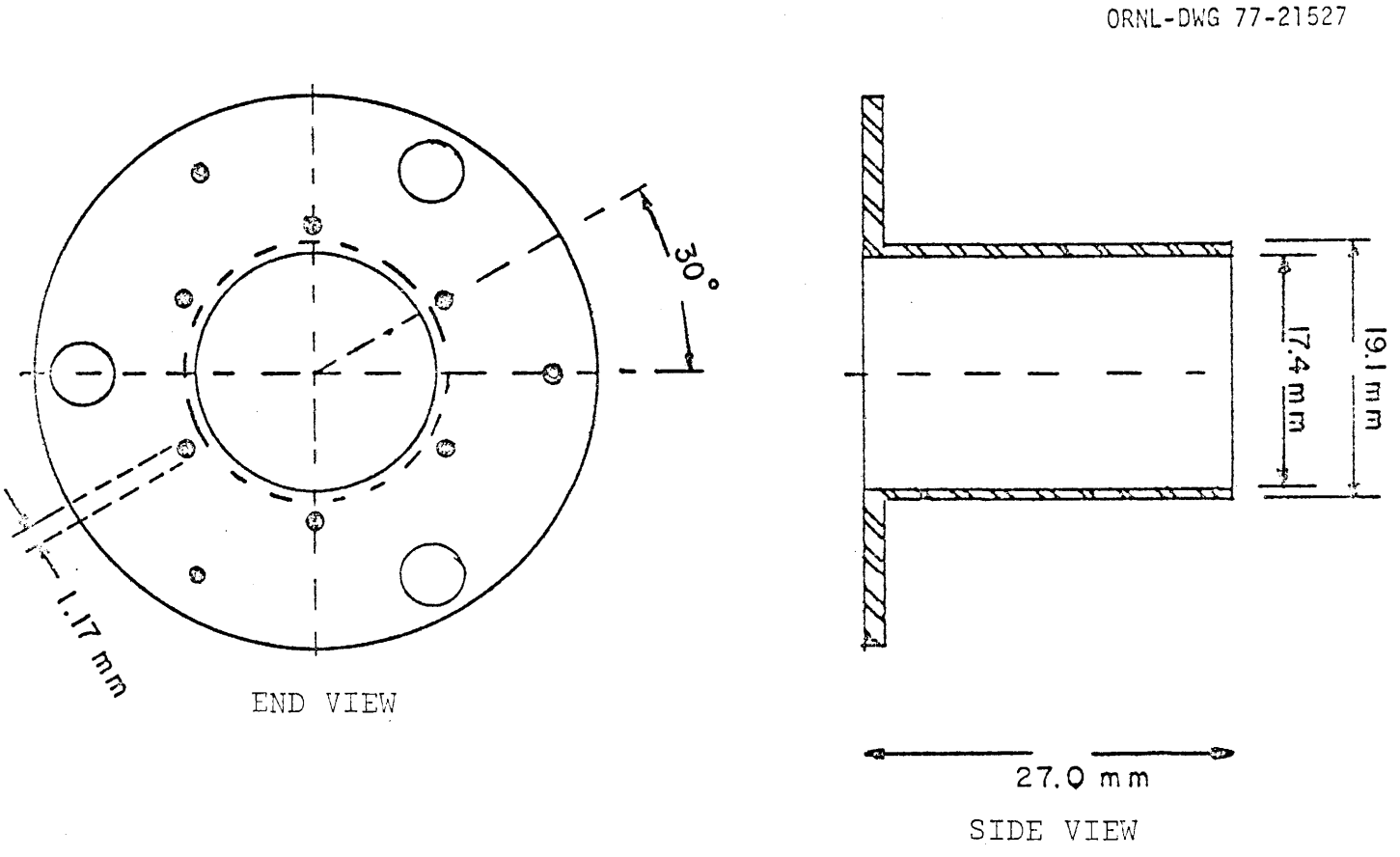

Figure IV-6. Schematic diagram of the inner cylinder.

electrodes (R). These retarding electrodes prevent any small angle scattered current from reaching the collector.

The collector, (7), and shield, (6), are maintained at the same potential (+ 15 volts with respect to the center filament). This is accomplished by two battery powered circuits which maintain a fixed potential while collecting the desired current. The current from the collector (7) is then fed into the preamplifier of the phase sensitive detection unit.

All electrodes, dees, collision chamber, and Faraday cup are of oxygen-free, high conductivity copper. Each was gold plated and coated with a thin graphite coating prior to assembly.

The entire apparatus was assembled with non-magnetic stainless steel screws with sapphire spacers (1.59 mm diameter spheres) to maintain proper alignment and to provide electrical insulation. The spacers were placed in the outer six holes of each electrode (FigureIV-2) with the assembled apparatus shown in Figure IV-1.

Scan Unit

A linear voltage ramp generator (scan unit) was designed and constructed at our laboratory to provide constant potentials, with respect to center filament, on all of the electrodes (1) through (7) and (16). The potential of the collision chamber and inner cylinder was monotonically increased to provide the linear change in the beam energy in

the interaction region. A typical scan was 0.0 to 7.5 volts at a rate of 1 volt per minute.

The potential of the collision chamber was monitored and fed into the X - input of an X - Y recorder (Hewlett-Packard Model 7004A). A block diagram of the operating system is shown in Figure IV-7.

Lock-In Amplifier and the Derivative Technique

A phase sensitive detection unit (Lock-In Amplifier) producing a sinusoidal signal with a peak-to-peak voltage of approximately 20mV at a frequency of 740 sec^{-1} is used to modulate the potential of the cylinder inside the collision chamber. This is referred to as the reference signal.

The current collected at the Faraday cup is fed to the input (preamplifier) of the Lock-In Amplifier. The phase-sensitive detection feature of the Lock-In Amplifier thereby accepts only a signal which has the same frequency and phase as the reference signal. Thus, for no change in the transmitted current, with changing electron energy, there is no signal produced at the Lock-In Amplifier output. If there is a variation in current with electron energy then the Lock-In Amplifier responds with a direct current signal proportional to that change. This technique produces a signal from the Lock-In Amplifier which represents the derivative of the electron current with respect to electron energy. This procedure, known as the "derivative technique," was first used in electron transmission spectroscopy by Sanche and Schulz.

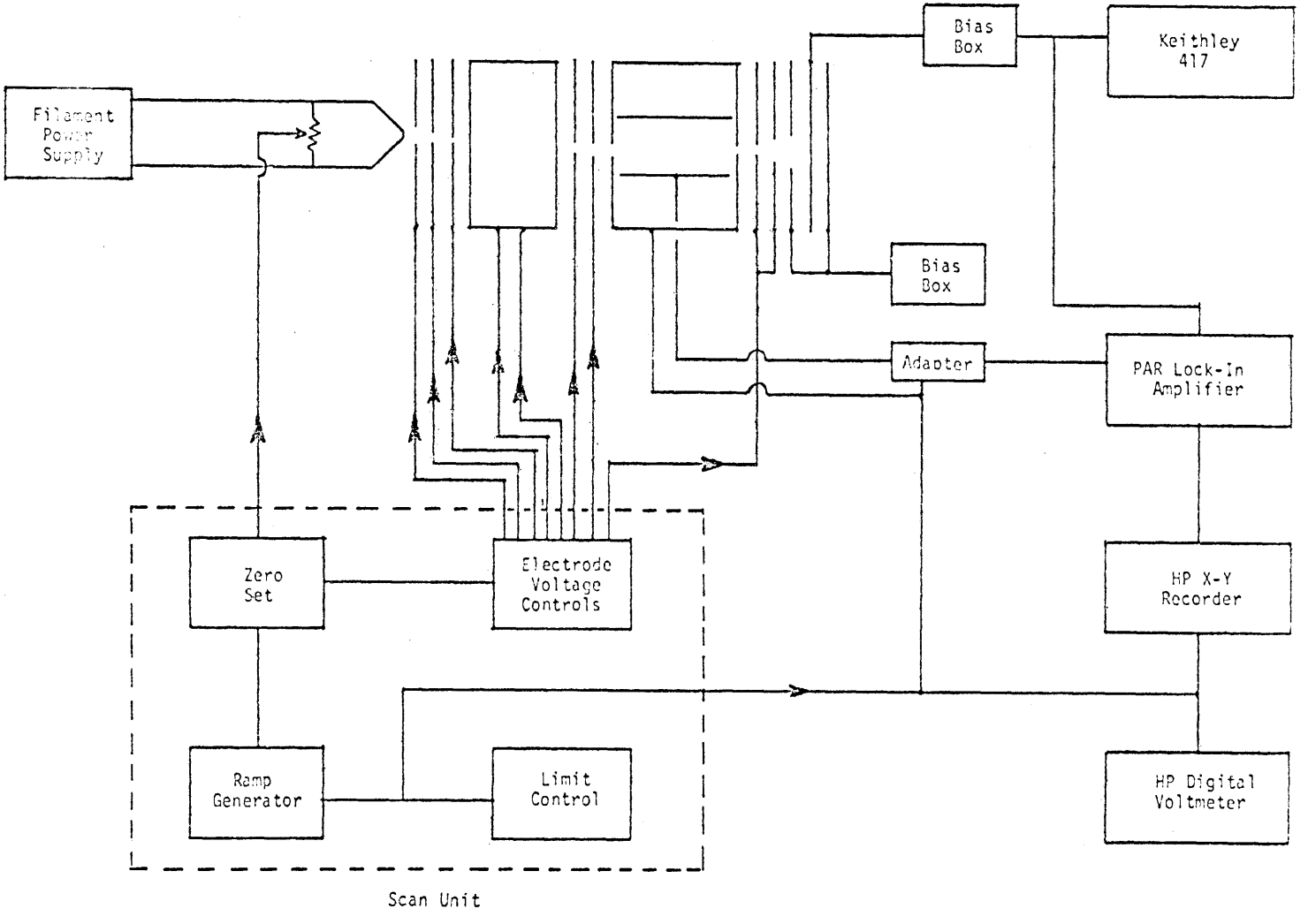

Figure IV-7. Block diagram illustrating the relationship between the electronic components and the components of the TEM.

To understand how this technique can produce information about electron-molecule interactions and, specifically, NIR's in gases, let us consider the following (after Sanche and Schulz, 1971). An incident electron current, I_o, passes into a sample gas of number density, N, with total electron scattering cross section σ_t. Only a portion of the electron current will exit the gas without interaction. After a length, l, through the collision region the transmitted current, I, is given by

$$I = I_o \; e^{-N\sigma_t l}$$

For a modulation of the electron energy $\Delta\varepsilon$, we have

$$\frac{\Delta I}{\Delta\varepsilon} = -I_o \frac{Nl\Delta(\sigma_t)}{\Delta\varepsilon} e^{-Nl\sigma_t} .$$

Thus, for small changes in σ_t as a function of ε, we have

$$\frac{\Delta I}{\Delta\varepsilon} \propto \frac{\Delta\sigma_t}{\Delta\varepsilon} .$$

The derivative technique greatly enhances sharp variations in I(E) such as those due to NIR formation (as well as vibrational structure on NIR's). This enhancement is shown in Figure IV-8 as $I(\varepsilon)$ and $\frac{dI}{d\varepsilon}$ are compared for N_2.

One major difficulty of this technique is its inability to detect very broad structures in the cross-section. This has been pointed out by Sanche and Schulz (1971) and by Mathur and Hasted (1976).

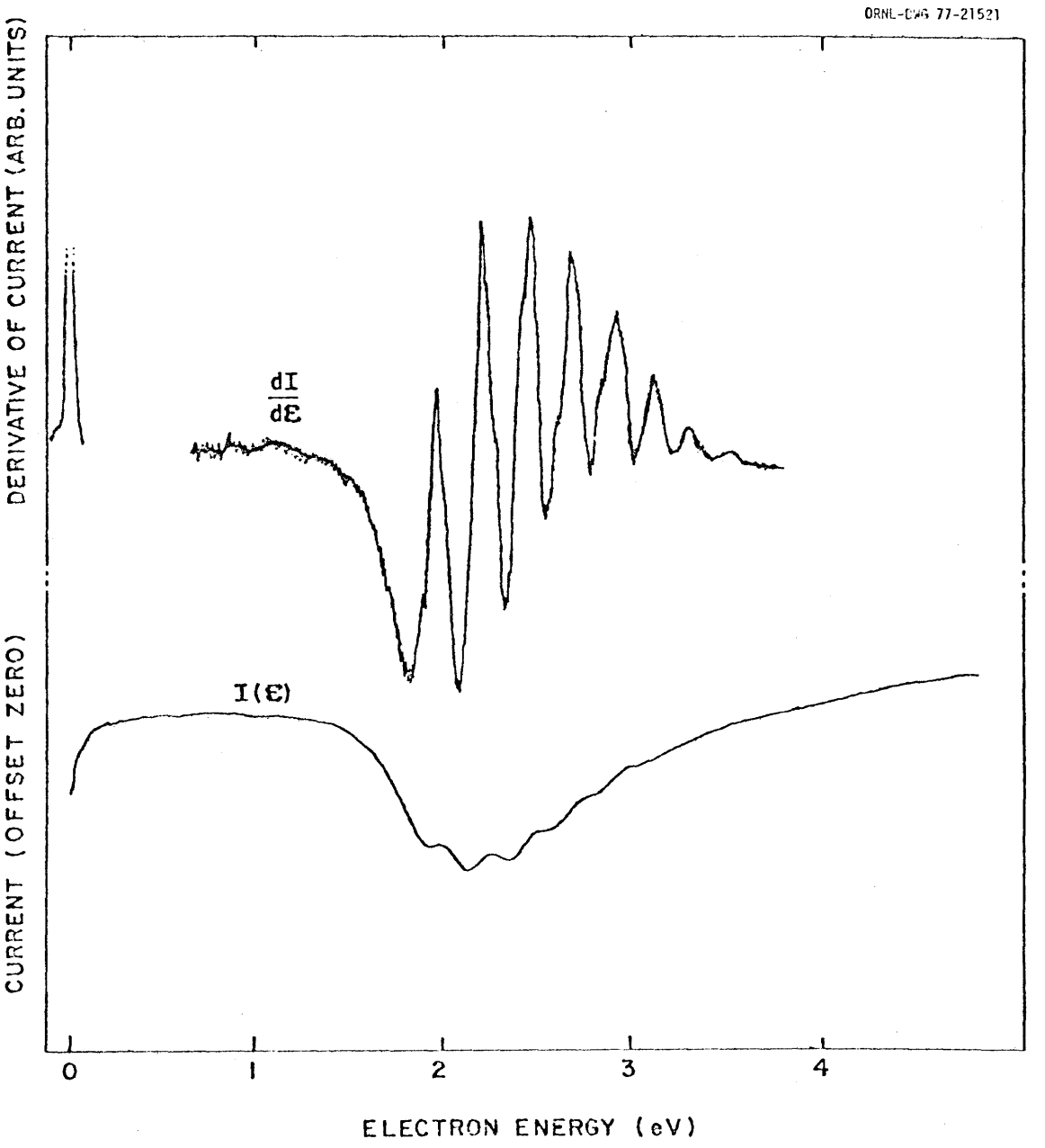

Figure IV-8. Electron transmission spectra of N_2 illustrating enhancement of structure by use of the derivative technique.

Magnetic Field

As mentioned earlier in this chapter the TEM operates in an axial magnetic field. The aligning magnetic field is produced by a long solenoid with the TEM coaxial with it and at its center. This solenoid is exterior to the main vacuum chamber.

The solenoid is 68. cm long with a mean diameter of 13.5 cm. There are 4790 turns of copper wire (with a diameter of 1.4 mm). A plot of the axial magnetic field, B, at the center of the solenoid as a function of the current through the coils, I, is shown in Figure IV-9. In Figure IV-10, the axial field, B, versus axial position is shown. The large region of uniformity in B can be seen from this plot.

Current for the solenoid is supplied by a regulated power supply (Sorenson Model DCR300.9B). A current of 0.0 to 9.0 A with a ripple factor $\sim$0.25% produces a magnetic field 0.0 to 765. Gauss at the center of the solenoid.

Alignment of the solenoid axis with respect to the axis of the TEM is accomplished by four set screws equally spaced around each end of the solenoid.

Vacuum System and Sample Manifold

A schematic diagram of the entire experimental apparatus is given in Figure IV-11. The main vacuum chamber contains the TEM, collision chamber and current collector. This chamber is pumped by a CVC four-inch oil diffusion pump (4) backed by a mechanical pump (1) (Welch Duo Seal, Model 13),

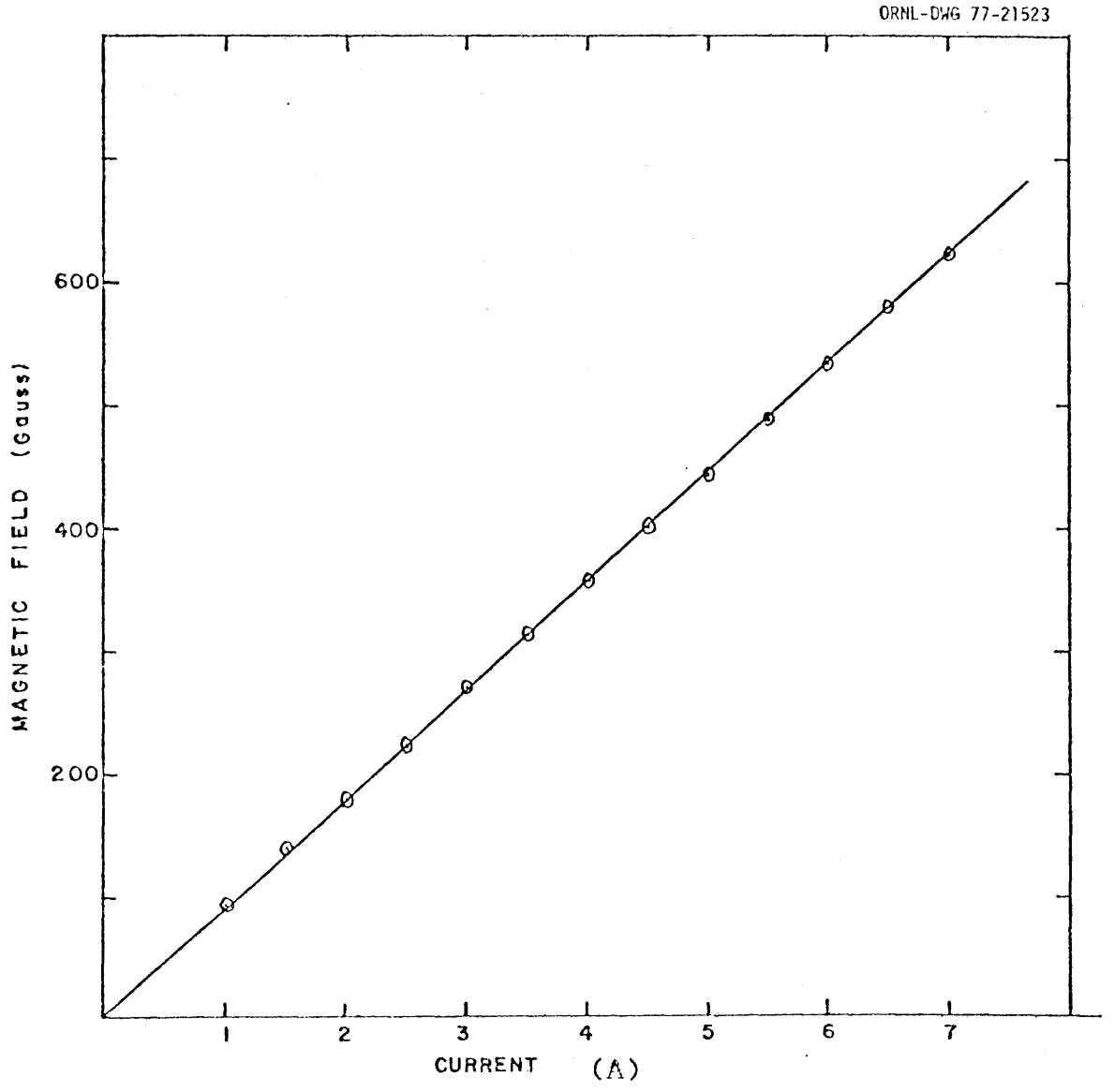

Figure IV-9. Plot of the measured magnetic field strength as a function of solenoid current.

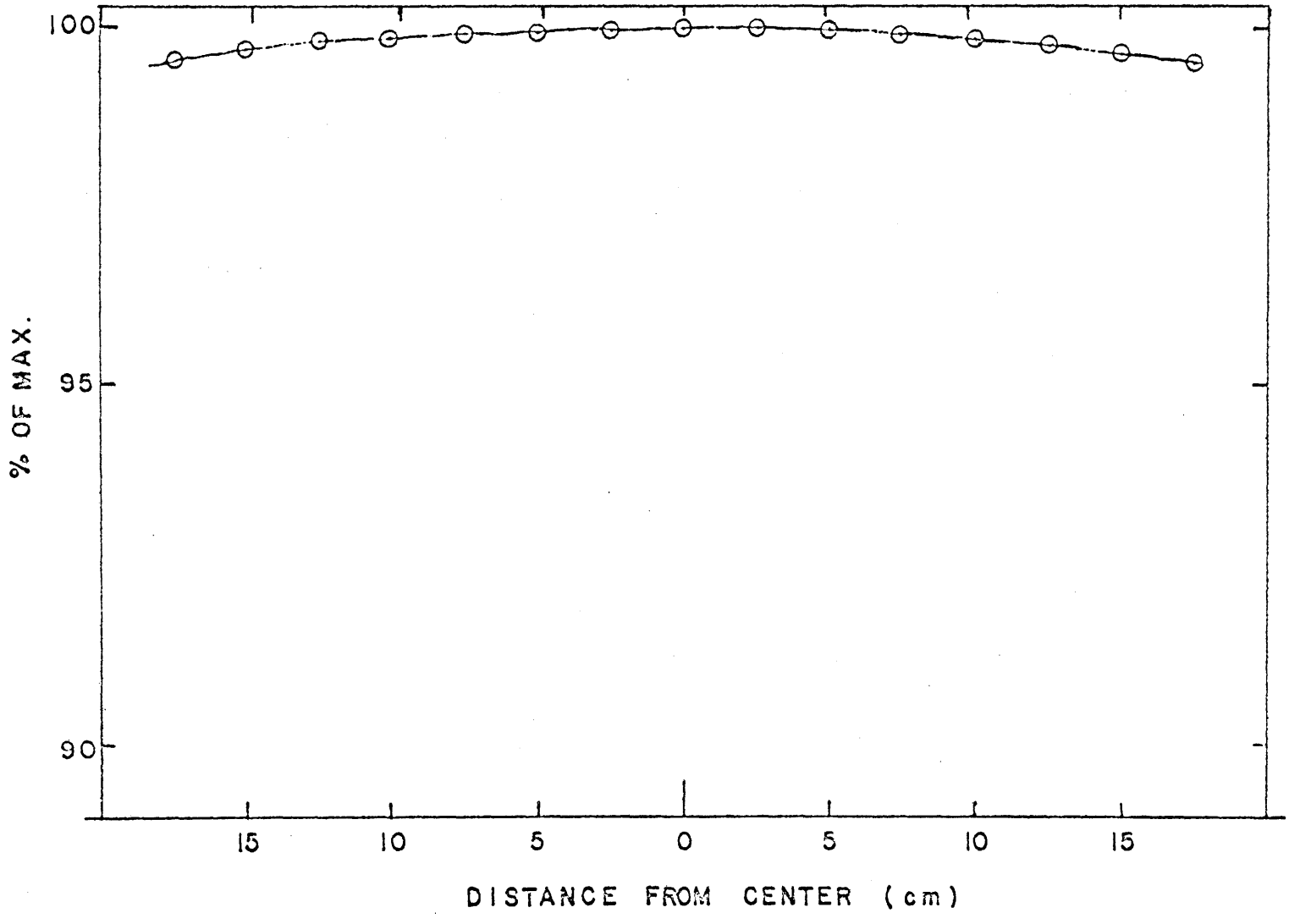

Figure IV-10. Measured uniformity of the magnetic field strength along the axis of the solenoid.

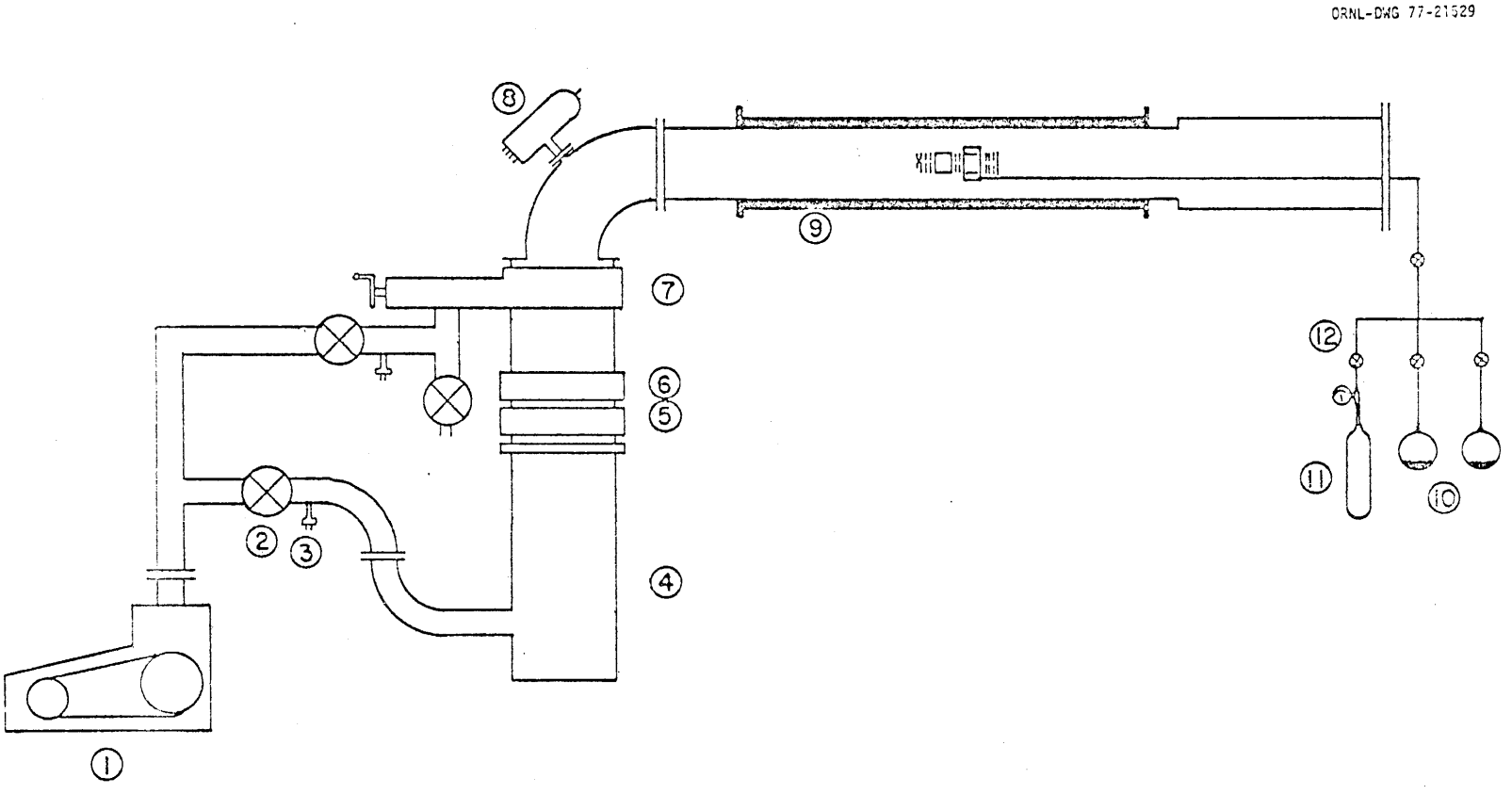

Figure IV-11. Schematic diagram showing the vacuum system and the position of the TEM inside the solenoid.

The foreline pressure is measured by a thermocouple gauge (3). An ionization gauge (8) (Veeco, Model RG-75K) measures the main chamber pressure. This gauge also serves as the pressure monitor for the sample gas during operation of the unit.

A CVC freon baffle (5) (type BCRW 21) and a CVC liquid nitrogen baffle (6) (41B) are connected between the main chamber and diffusion pump to minimize backstreaming of pump oil vapors into the main chamber. A CVC fine pressure valve (7) (VCS-41B) allows for isolation of the main chamber from the pumping system.

This vacuum system provides a chamber pressure of the order of 10^{-9} torr following bakeout and prior to admission of the sample gas. The pressure (at the ion gauge) is increased to 10^{-3} torr to 10^{-5} torr during sample gas-flow conditions.

The sample manifold is a triple-input, single-output junction of welded stainless steel tubing (6.35 mm diameter). This permits mixing of the sample with reference gases during operation. Nitrogen and benzene are the usual reference gases whereas argon and nitrogen are used as absolute energy calibrants.

Metering valves (12) (Hoke, Inc.) were used to control gas flow into the collision chamber. Changes in pressure were carefully monitored during each scan.

Energy Calibration

Due to the nature of the experiment there are contact potentials and other factors which cause the scan unit voltage reading (collision chamber voltage) to differ from the absolute electron energy. Argon, with a sharp resonance at 11.064 - 11.094 eV (Kuyatt et al., 1965), was used as an energy scale calibration gas. The first minimum of the N_2 resonance 1.89 eV (Ehrhardt and Willmann, 1967) was also used for energy scale calibration. These two energy calibrations provided a linearity check of the measured values of the electron beam energy.

Each value of the electron beam energy which was measured from the scan unit voltage readings was adjusted to correspond to published values for the energy of structure observed in the calibration gases. A verification of the helium resonance at 19.30 - 19.37 eV (Sanche and Schulz, 1971) further justified our calibration procedure.

Each scan of the fluorobenzenes and biphenyl was preceded by a scan with no gas present (i.e. vacuum of $\sim 10^{-9}$ torr) as a first check for instrumental effects. The derivative of the transmitted current was monitored for the voltage range of 0.0 - 7.5 volts. Particular emphasis was placed on the onset of the beam (i.e. retarding curve). The full-width-at-half-maximum (FWHM) of this curve gave a lower bound to the resolution of the apparatus. Typically this was between 15meV and 25meV (from scan unit voltages). An upper bound can be assigned as approximately 50 meV by

observing known structure which can be resolved to a full width at half maximum of this magnitude. From the uncertainties we have just discussed we conclude that the probable error in absolute energy assignment for vibrational structure is ∿0.04 eV for the determination of EA's and ∿0.06 eV for the determination of VAE's.

Following each fluorobenzene or biphenyl scan, a scan of nitrogen was made to determine the location of the first vibrational structure on the 2.3 eV N_2^- shape resonance. Corrections were made with respect to this 1.89 eV (Ehrhardt and Willmann, 1967) energy position. This procedure was varied from time to time to check for residual molecules not evacuted between scans.

IV. SUMMARY

The TEM electron transmission device we have built has proven to be a valuable tool with which negative ion resonances of polyatomic molecules can be studied and their electron affinities and/or vertical attachment energies can be determined.

Obvious difficulties in the experimental procedure are poisoning of the filament by the sample gas and precise energy calibration. Spurious structure often observed in this type of experiment was discounted by varying the magnetic field. In this way, all (or nearly all) of the spurious structure varied in their energy locations while "true" structure remained fixed in its energy dependence.

CHAPTER V

NEGATIVE ION RESONANCES OF BENZENE

I. INTRODUCTION

The importance of negative ion formation involving biologically important molecules has prompted the present investigations of benzene--the basic building block of many organic compounds. Analysis of negative ion resonances of benzene provided information concerning the fundamental physical processes involved in low-energy electron interactions with these molecules. Information obtained from the present work is of use to the organic chemist, the radiation biochemist, as well as to the radiation physicist.

II. BRIEF THEORY

The benzene molecule is known to be planar and to have a regular hexagonal structure with a carbon atom at each vertex. A single hydrogen atom is bonded to each carbon atom. The chemical expression for benzene is thus C_6H_6 and benzene has point group symmetry D_{6h}.

Molecular orbital theory requires that of the 42 electrons belonging to the benzene molecule, 12 are in C-H bonding orbitals, 24 are in extended σ orbitals of the ring, and six are in π orbitals perpendicular to the plane of the molecule. The six π electrons fill the three lowest π orbitals shared by the carbon atoms (Bardsley and Mandl, 1968).

The six π orbital wave functions for benzene are normally labeled $\psi_1, \psi_2, \psi_3, \psi_4, \psi_5$ and ψ_6 with corresponding orbital energies $\varepsilon_1, \varepsilon_2, \varepsilon_3, \varepsilon_4, \varepsilon_5$ and ε_6. By symmetry arguments we have $\varepsilon_1 < \varepsilon_2 = \varepsilon_3 < \varepsilon_4 = \varepsilon_5 < \varepsilon_6$ (Christophorou, et al. 1977). The configuration of the neutral benzene molecule in its ground state is $(a_{2u})^2 (e_{1g})^4 \, {}^1A_{1g}$ where the six π orbitals are termed a_{2u}, e_{1g}, e_{2u}, and b_{2g} according to group terminology. We shall refer to these orbitals as the π_1, π_2, π_3, π_4, π_5, and π_6 orbitals, respectively. The neutral benzene molecule in its ground state has the π_1, π_2, and π_3 orbitals filled. A more complete discussion of the π electron structure of benzene is given by Christophorou (1971).

Theoretical treatments of the molecular orbitals for negative ion formation in benzene treat the π orbitals separate from the σ electron network. Within this framework the ground state of the benzene negative ion is expected to be $(a_{2u})^2 (e_{1g})^4 (e_{2u}) \, {}^2E_{2u}$. Due to the symmetry of the molecule, the symmetric and antisymmetric e_{2u} orbitals are experimentally indistinguishable so that the additional electron going into either π_4 or π_5 orbital yields one NIR.

The configuration $(a_{2u})^2 (e_{1g})^4 (b_{2g}) \, {}^2B_{2g}$ represents an extra electron going into the π_6 orbital of the ground state of the benzene molecule (Mathur and Hasted, 1976). Other configurations correspond to excited states of the molecular negative ion and are not <u>shape</u> resonances.

III. EXPERIMENTAL RESULTS

A negative ion resonance of the benzene molecule was first detected by Compton et al. (1966) using the SF_6 scavenger technique (see Chapter III). Vibrational structure on the resonance was observed by Boness et al. (1967) thus permitting a determination of the EA of the isolated molecule. Boness et al. (1967) attributed the vibrational structure that they observed to the C--C stretching mode of the neutral molecule.

Sanche and Schulz (1973) obtained high resolution electron transmission spectra which showed a marked anharmonicity of the vibrational structure. They assigned the vibrational mode to the totally symmetric "ring breathing," or ν_2, mode which is observed in the neutral molecule (Herzberg, 1966). A broad structure in the spectra at higher energies was detected (Sanche and Schulz, 1973) which was interpreted as a shape resonance associated with a higher angular momentum state.

In the present work electron transmission spectra for benzene vapor were obtained using a TEM described in Chapter IV. A typical transmission spectrum is shown in Figure V-1.

Comparison of the assignment and the positions of the observed negative ion resonances of benzene is presented in Table V-1 while a comparison of the electron transmission data for the lowest NIR of benzene is presented in Table V-2.

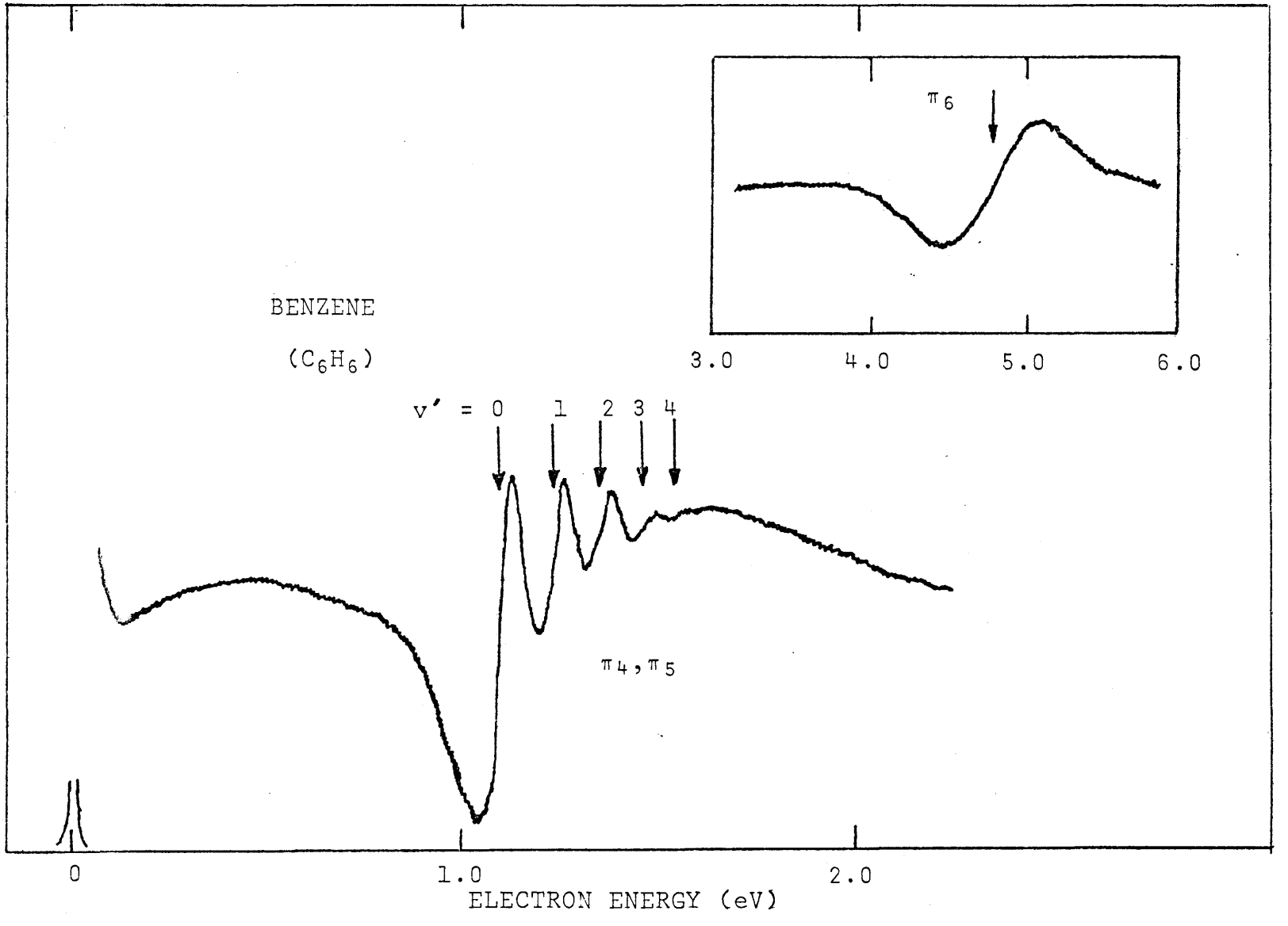

Figure V-1. Electron transmission spectrum of benzene showing vibrational structure.

TABLE V-1

ASSIGNMENT AND POSITION OF THE OBSERVED NIR'S OF BENZENE

Position of Resonance (eV) π_4, π_5	π_6	Other Structure (eV)	Reference	Method
(+1.40)*	- - -	- - -	Compton et al. (1966)	SF_6 Scavenger
(+1.35)	- - -	- - -	Hubin-Franskin and Collin (1970)	SF_6 Scavenger
+1.14 ± 0.05**	(+4.80 ± 0.05)	- - -	Sanche and Schulz (1973)	Electron Transmission Derivative Technique
+1.15 ± 0.05	(+4.85 ± 0.08)	- - -	Jordan et al. (1976)	Electron Transmission Derivative Technique
+1.086 ± 0.03	(+4.93 ± 0.03)	(+4.21 ± 0.03) (+8.85 ± 0.05)	Mathur and Hasted (1976)	Electron Transmission Derivative Technique
+1.13 ± 0.04	(+4.80 ± 0.06)	- - -	Present work	Electron Transmission Derivative Technique

*Each value in parentheses is the position of the maximum of the NIR (i.e. the VAE). Values not in parentheses are the positions of the first vibronic levels of the NIR.

**Error in absolute energy assignment.

TABLE V-2

COMPARISON OF DATA ON THE LOWEST NIR OF BENZENE

Position of first vibronic level (eV)	Mean Vibrational Spacing (eV)	Vibrational Spacings (eV)	Anharmonicity (eV)	Reference
1.15 ± 0.05*	0.12 (3)**	- - -	- - -	Boness et al. (1967)
1.07 ± 0.07	0.127***	- - -	- - -	Larkin and Hasted (1972)
1.14 ± 0.05	0.115 (4)	0.123 v′=0 - v′=1		Sanche and Schulz (1973)
			0.005	
		0.118 v′=1 - v′=2		
			0.006	
		0.112 v′=2 - v′=3		
			0.006	
		0.106 v′=3 - v′=4		
1.086 ± 0.03	0.114 (4)	0.120 v′=0 - v′=1		Mathur and Hasted (1976)
			0.004	
		0.116 v′=1 - v′=2		
			0.006	
		0.112 v′=2 - v′=3		
			0.005	
		0.107 v′=3 - v′=4		

TABLE V-2 (continued)

Position of first vibronic level (eV)	Mean Vibrational Spacing (eV)	Vibrational Spacings (eV)	Anharmonicity (eV)	Reference
1.13 ± 0.04	0.116 (4)	0.128 $v'=o - v'=1$		Present work
			0.008	
		0.120 $v'=1 - v'=2$		
			0.008	
		0.112 $v'=2 - v'=3$		
			0.007	
		0.105 $v'=3 - v'=4$		

*Error in absolute energy assignment.

**Number of levels spacings averaged.

***v=0 to v=1 level only.

All values for the position of the first vibronic level (which give a measure of the EA) in Table V-2 are in agreement (within experimental error). The present results exhibit somewhat greater anharmonicity than in earlier referenced work but again these are within the experimental accuracy of the experiments.

It is worth noting that additional structure observed by Mathur and Hasted (1976) was not observed in the present experiment. Other authors who also failed to observe this structure are listed in Table V-1 (p. 58). This could be due to differences in signal enhancement techniques.

Averaging data taken under various experimental conditions we have arrived at the value of -1.13 ± 0.04 eV for the EA of the π_4, π_5 degenerate orbitals. Vertical attachment energies are determined to be -1.37 ± 0.06 eV for the π_4, π_5 degenerate orbitals and -4.80 ± 0.06 eV for the π_6 orbital.

In Table V-3 a summary of pertinent information for benzene is presented. The vibrational modes of the positive ion, neutral molecule, and negative ion indicate that our qualitative description of the extra electron as being in a path of large radial dimensions is valid. The addition or removal of an electron from the neutral benzene molecule apparently has little effect on the dominant vibrational mode of the molecule.

In Chapter II the relationship between the resonance energy, resonance width, and the ℓth partial wave cross

TABLE V-3

PERTINENT INFORMATION FOR BENZENE

Ionization Energies (eV)		Electron Affinities** (eV)		Vibrational energies		
π_1	π_2, π_3	π_4, π_5	π_6	positive ion (meV)	neutral (meV)	negative ion (meV)
$(12.3)_1$*	9.241_2	$(-1.40)_4$	$(-4.80)_6$	122_2	123_3	127_7
$(12.1)_{12}$	$(9.40)_{11}$	$(-1.35)_5$	$(-4.85)_8$			123_6
		-1.14_6	$(-4.93)_9$			120_9
		-1.15_8	$(-4.80)_{10}$			128_{10}
		-1.086_9				
		-1.13_{10}				
		-1.07_7				

TABLE V-3 (continued)

*Ionization energies in parentheses are vertical values.
Ionization energies not in parentheses are adiabatic values.

**Values not in Parentheses are true (adiabatic) electron affinities.
Values in parentheses are vertical attachment energies.

***Vibrational mode identified as ring breathing mode, v_2.
Energies shown are $v_2=0 - v_2=1$.

Bibliography for Table V-3.

1. Brundle, et al. (1972)
2. Asbrink, et al. (1970)
3. Herzberg (1945)
4. Compton, et al. (1966)
5. Hubin-Franskin and Collin (1970)
6. Sanche and Schulz (1973)
7. Larkin and Hasted (1972)
8. Jordan, et al. (1976)
9. Mathur and Hasted (1976)
10. Present work
11. Baker, et al. (1968)
12. Narayan and Murrell (1970)

section was presented:

$$\sigma_{\ell} = \frac{4\pi}{k^2}(2\ell+1)\sin^2\left(\delta_0(k)+\tan^{-1}\frac{\frac{1}{2}\Gamma_{\ell}}{\varepsilon_{R\ell}-\varepsilon}\right) \quad . \qquad \text{II-15}$$

Since $k^2 = \frac{2m\varepsilon}{\hbar^2}$ we have

$$\sigma_{\ell} = \frac{4\pi\hbar^2}{2m\varepsilon}(2\ell+1)\sin^2\left(\delta_0(k)+\tan^{-1}\frac{\frac{1}{2}\Gamma_{\ell}}{\varepsilon_{R\ell}-\varepsilon}\right) \quad . \qquad \text{V-1}$$

We use experimental values for Γ_{ℓ} and $\varepsilon_{R\ell}$ for the π_6 resonance of benzene to approximate the maximum partial wave cross section for ε slightly less than $\varepsilon_{R\ell}$. Taking $\ell = 4$ (Sanche and Schulz, 1973) and using

$\Gamma_4 \simeq 0.63$ eV

and $\varepsilon_{R4} = 4.8$ eV we can find σ_4 from Equation V-1. Let $\delta(k) = 0$ for simplicity and since no appreciable cross section is noted far from the resonance position.

We thus have

$\sigma_{4\,max.} \sim 89. \times 10^{-16}$ cm^2 .

In order to obtain an order of magnitude for the lifetime of this resonance we use the uncertainty principle $\tau_{\ell} = \frac{\hbar}{\Gamma_{\ell}}$. For the π_6 resonance of benzene we have $\Gamma_4 \sim 0.63$ eV which yields an approximate lifetime of the resonant state of $\tau_4 \sim 10^{-16}$ sec.

IV. SUMMARY

The primary purpose of the present electron transmission studies of benzene was to insure the correct operation of the experimental apparatus and to confirm the experimental results of other research groups. Upon completion of this

task, spectra of fluorobenzenes were taken which will be discussed in Chapter VI. In Chapter VII transmission spectra of biphenyl are presented, analyzed, and discussed.

CHAPTER VI

NEGATIVE ION RESONANCES OF FLUOROBENZENES

I. INTRODUCTION

The importance of negative ion resonances of benzene has already been mentioned (Chapter V). The next series of molecules of this type that one can consider are the substituted benzene derivatives. These molecules provide a progression in the complexity of molecules considered in our investigation of low-energy electron interactions with biologically important molecules. Although negative ion resonances of benzene derivatives have been reviewed in recent literature (Christophorou et al., 1977) there has never been a systematic investigation of negative ion resonances for a complete series of benzene derivatives with a common substituent. Fluorine has been chosen as the common substituent for the present investigation for several reasons:

1. Most fluorobenzene compounds are commercially available.
2. Fluorine is the most electronegative atomic species.
3. Fluorine-containing compounds are important in engineering, physical sciences, and medicine.
4. There are no complications due to dissociative attachment at low energies.

In the present work the following fluorobenzenes are

studied: fluorobenzene (C_6H_5F): 1,4-difluorobenzene (1,4-$C_6H_4F_2$); 1,3,5-trifluorobenzene (1,3,5-$C_6H_3F_3$); 2,3,5,6-tetrafluorobenzene (2,3,5,6-$C_6H_2F_4$); pentafluorobenzene ($C_6H\ F_5$); and hexafluorobenzene (C_6F_6). The enumeration pattern of each compound indicates the location of the fluorine substituents on the benzene ring. This is illustrated in Figure VI-1.

Curran (1963) first obtained energy loss spectra of fluorobenzene by use of the SF_6 scavenger technique (see Chapter III). The interpretation of the structure in the energy loss spectra of fluorobenzene as due to a negative ion resonance was made a few years later by Compton, et. al. (1966). Naff and co-workers (1968) studied a series of fluorobenzene compounds and concluded that a linear relationship existed between the number of fluorine substituents and the vertical attachment energy of these molecules.

Christophorou et. al. (1974) detected two negative ion resonances for fluorobenzene vapors using threshold-electron-excitation spectroscopy. More recently, Jordan, et al. (1976) performed electron transmission studies of fluorobenzene and found an additional negative ion resonance at higher energy as well as two negative ion resonances corresponding to those found by Christophorou et al. Jordan et al. also observed pronounced vibrational structure on the lowest-energy resonance.

Charge transfer reactions indicate that the electron

ORNL-DWG 77-21524

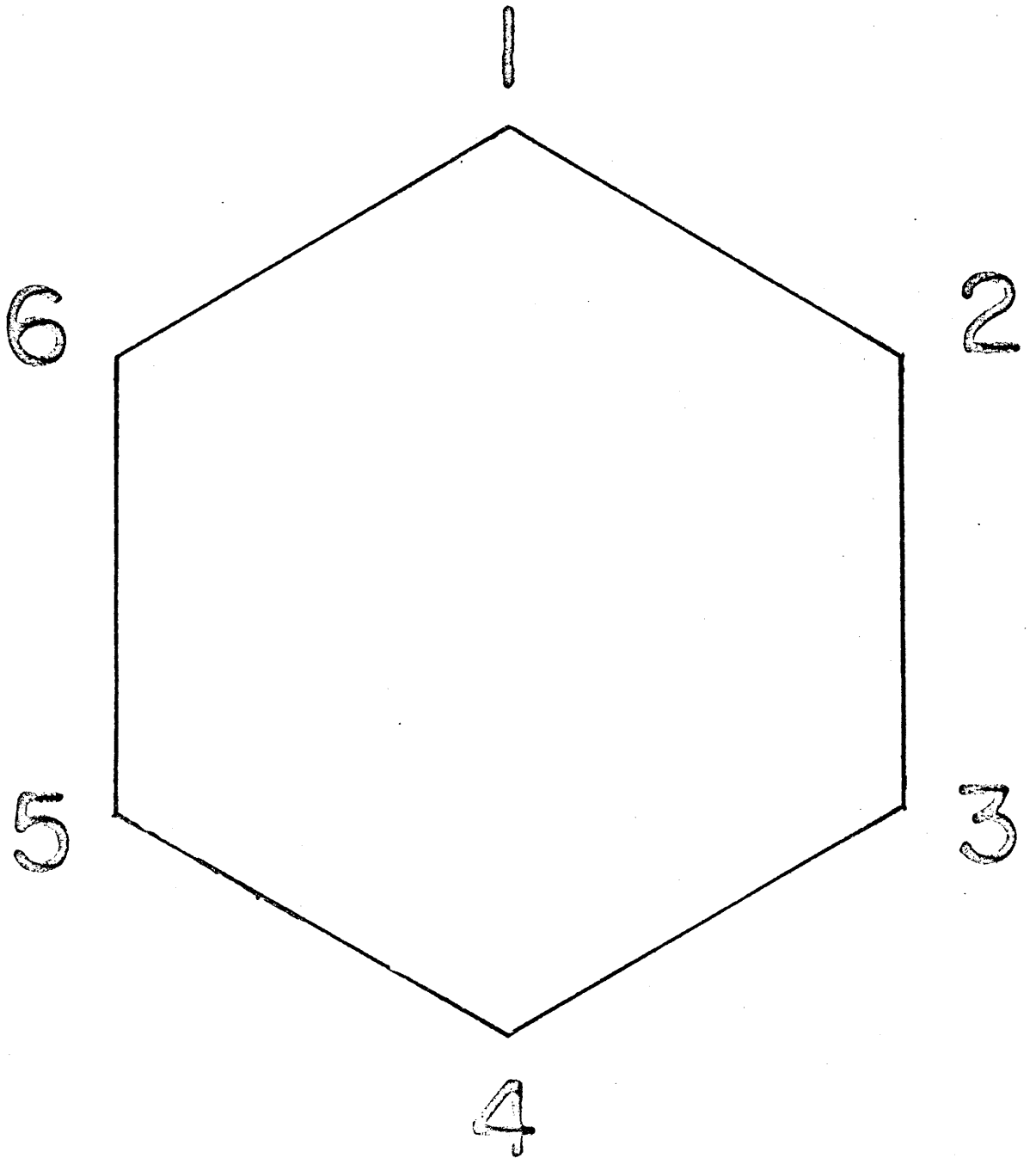

Figure VI-1. Diagram illustrating the enumeration scheme for the carbon atom positions on the benzene ring.

affinity of hexafluorobenzene is + 1.8 ± 0.3 eV (Lifshitz, et al., 1973). Chen and Wentworth (1975) have estimated the electron affinity of hexafluorobenzene to be + 1.20 ± 0.07 eV using the magnetron method. Gant and Christophorou (1976) detected an additional negative ion resonance in hexafluorobenzene at -0.73 eV in their swarm experiments. They further assigned this resonance to capture of an electron into the π_6 orbital of hexafluorobenzene (Gant and Christophorou, 1976).

The preceding experiments provided the background for the present work. When the complete series of fluorine substituted benzene derivatives are considered, new information as to the location and assignment of negative ion resonances of these molecules can be made.

II. PRESENT EXPERIMENTAL RESULTS

While the benzene sample was obtained from James Hinton, Newport News, Virginia, with a stated minimum purity of 99.999%, the fluorobenzenes were obtained from other sources with purities stated in Table VI-1.

Since all samples are liquids at room temperature (25°C) each sample was submitted to multiple freeze-pump-thaw cycles to remove trapped gases (mostly air). Each sample was attached to the apparatus in a glass flask (10) as shown on page 50. The compounds had sufficient vapor pressure so that no heating of the system was required. All spectra were obtained in the manner described in Chapter IV.

Figures VI-2 and VI-3 show electron transmission

TABLE VI-1

SOURCE AND PURITY FOR EACH
FLUOROBENZENE COMPOUND USED IN THIS WORK

Compound	Minimum Purity	Supplier
Fluorobenzene	99.%	Aldrich Chemical Company
1,4-difluorobenzene	98.%	Aldrich Chemical Company
1,3,5-trifluorobenzene	98.%	Peninsula Chemical Research, Inc.
2,3,5,6-tetrafluorobenzene	99.+%	Peninsula Chemical Research, Inc.
Pentafluorobenzene	99.+%	Peninsula Chemical Research, Inc.
Hexafluorobenzene	99.%	Aldrich Chemical Company

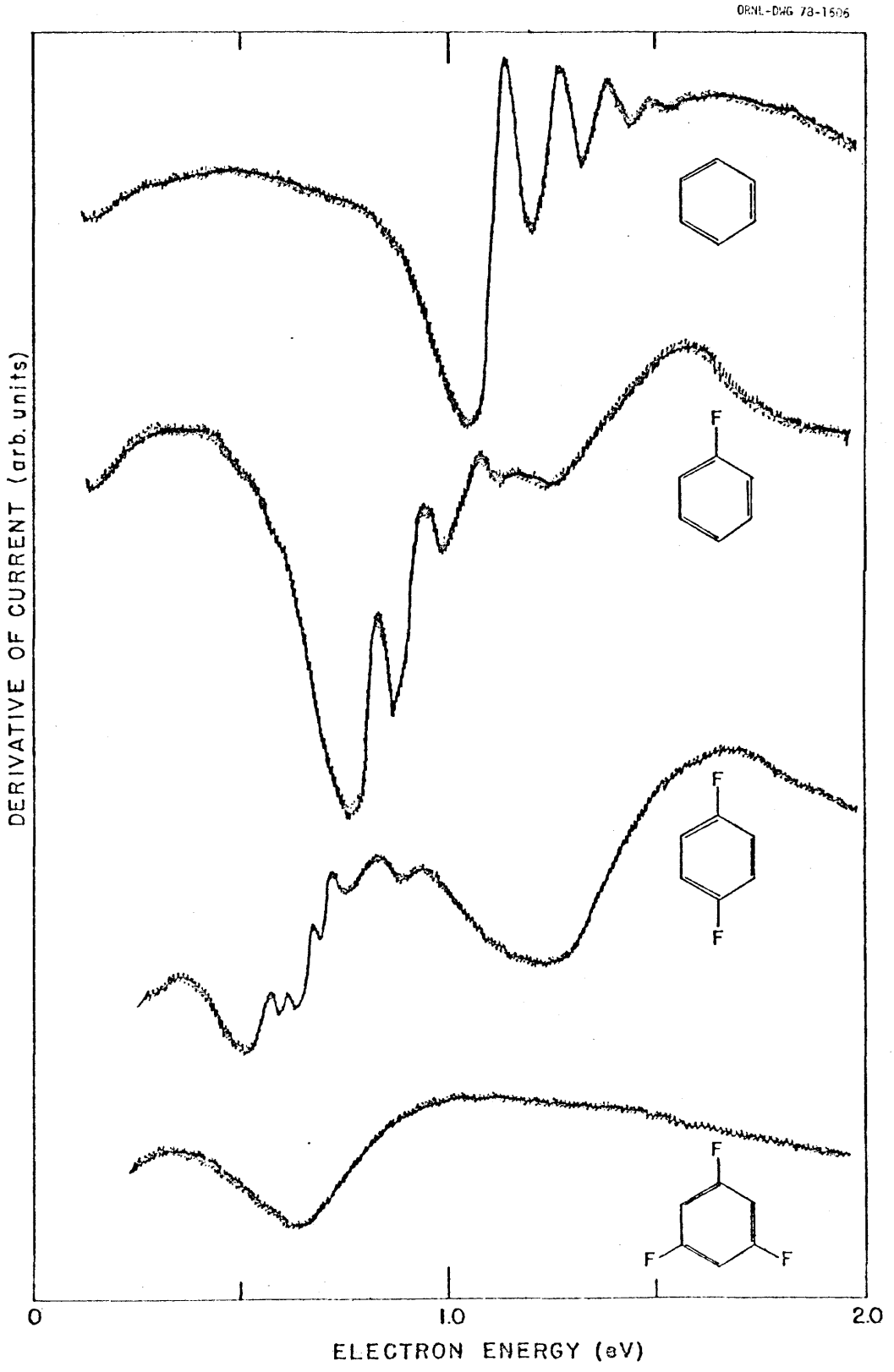

Figure VI-2. Electron transmission spectra for benzene, fluorobenzene, 1,4-difluorobenzene, and 1,3,5-trifluorobenzene.

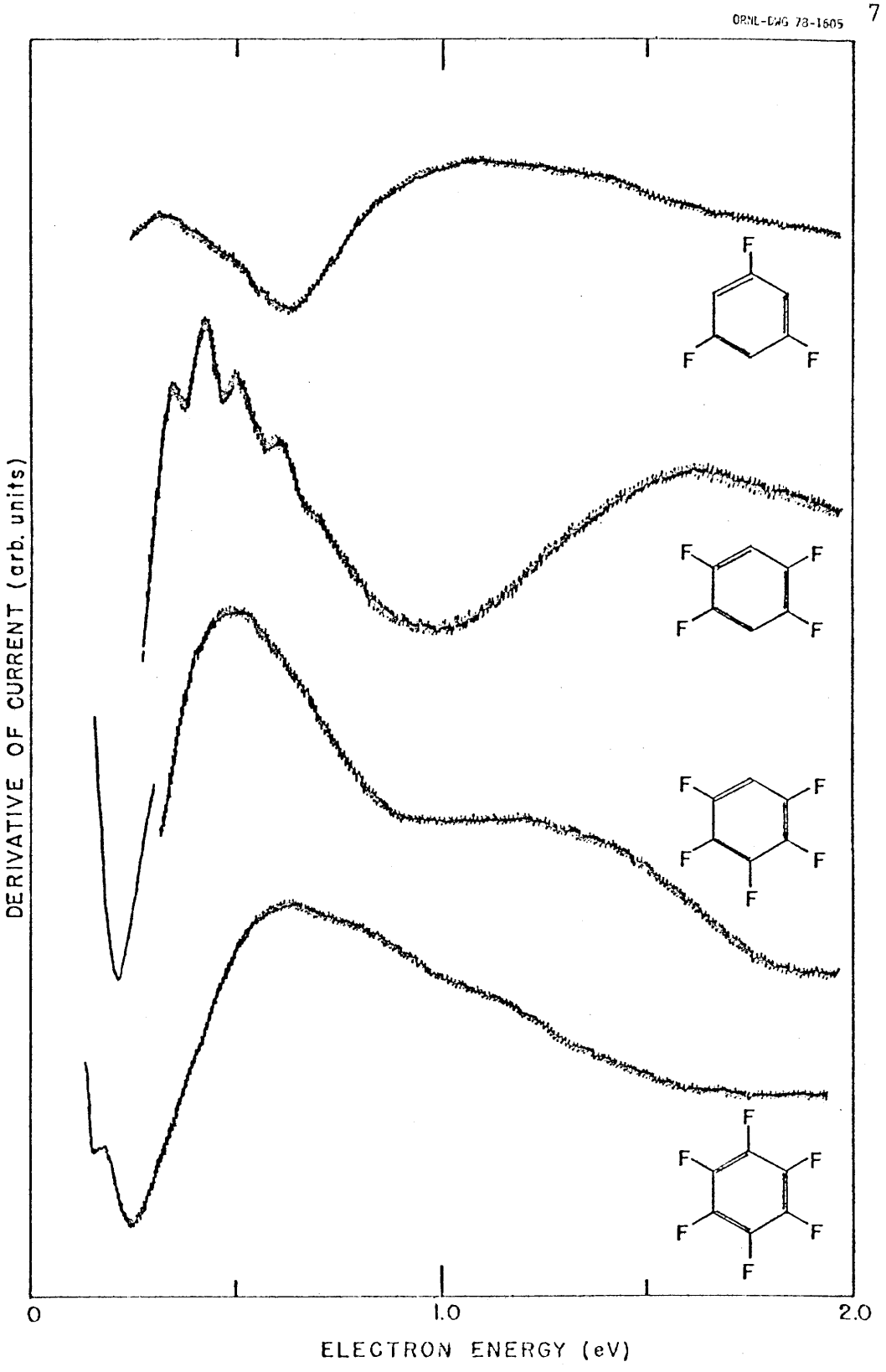

Figure VI-3. Electron transmission spectra for 1,3,5-trifluorobenzene, 2,3,5,6-tetrafluorobenzene, pentafluorobenzene, and hexafluorobenzene.

spectra (derivative technique) for benzene and six fluorobenzenes for incident electron energies from thermal to 2.0 eV. In Figure VI-4 we present the electron transmission spectra of the same compounds for incident electron energies from 2.0 to 7.0 eV. Interpretation of the electron transmission spectrum for each compound will be considered separately.

Fluorobenzene

Three pronounced structures are found in the transmission spectra of fluorobenzene (C_6H_5F). The first is centered at an incident electron energy of 0.91 ± 0.06 eV. Vibrational progressions are seen on this structure with the energy of the first vibrational maximum at 0.82 ± 0.04 eV. Vibrational spacings are found to increase in all C_6H_5F spectra. We assign this structure as being due to a NIR associated with electron capture into the π_4 orbital of the fluorobenzene molecule. The first π-electron affinity of the molecule is thus -0.82 ± 0.04 eV and the first π-vertical attachment energy is -0.91 ± 0.06 eV. The observed vibrational spacings are 0.113, 0.121, and 0.133 eV. These values are determined by measuring the energy spacing between successive midpoints of the fine structure. A midpoint is found as the point halfway between the minimum and maximum on the derivative curve. We postulate that the increasing vibrational spacings can be due to overlapping vibrational bands corresponding to the 0.100 eV symmetric mode (Smith et al., 1953) and the 0.125 eV symmetric mode (Clark and McCaffery, 1977) of the neutral molecule. A comparison of

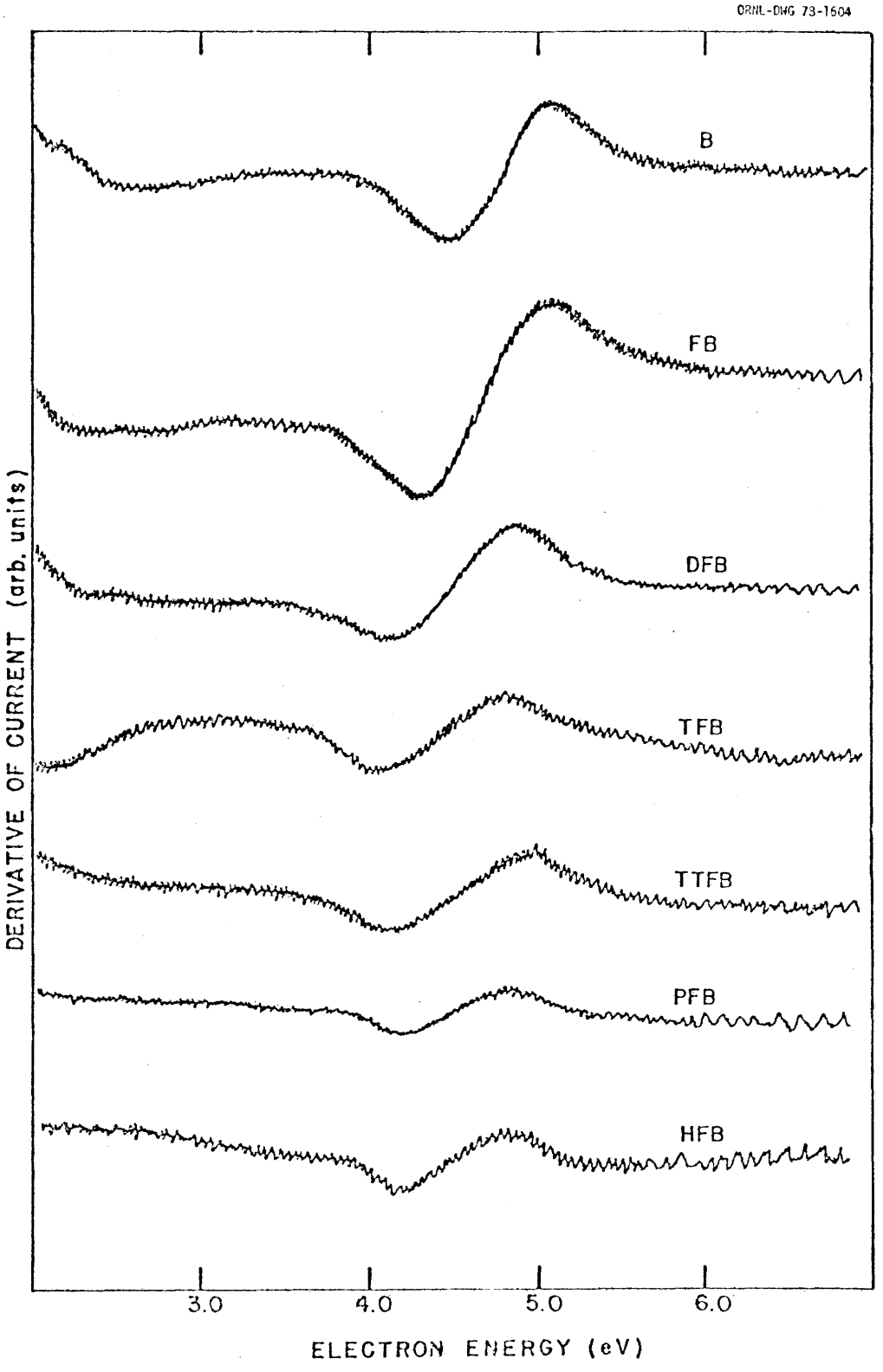

Figure VI-4. Electron transmission spectra for benzene (B), fluorobenzene (FB), 1,4-difluorobenzene (DFB), 1,3,5-trifluorobenzene (TFB), 2,3,5,6-tetrafluorobenzene (TTFB), pentafluorobenzene (PFB), and hexafluorobenzene (HFB).

the present experimental results for this NIR of C_6H_5F with the work of Jordan et al., (1976) is made in Table VI-2.

TABLE VI-2

COMPARISON OF DATA ON THE LOWEST NIR OF FLUOROBENZENE

Position of first vibronic level (eV)	Vibrational spacings (eV)	Reference
0.89 ± 0.05*	∿0.115 ∿0.113 ∿0.115	Jordan et al. (1976)
0.82 ± 0.04	∿0.113 ∿0.121 ∿0.133	Present work

*Error in absolute energies.

The second observed structure is centered at an incident electron energy of 1.40 ± 0.06 eV. There is no observed vibrational progression on this structure. This structure is attributed to the second negative ion resonance (π_5) with a vertical attachment energy of -1.40 ± 0.06 eV.

For incident electron energies above two electron volts only one structural pattern was observed in our transmission spectra C_6H_5F. This structure was very symmetric with no superimposed fine structure and was centered at 4.66 ± 0.06 eV. This is attributed to the third negative ion

resonance (π_6) with a vertical attachment energy of -4.66 ± 0.06 eV.

A summary of the assignment and positions of the negative ion resonances of fluorobenzene is given in Table VI-3.

Table VI-4 gives a listing of some pertinent information concerning C_6H_5F--for positive ions, neutral molecules, and negative ions. This information will be considered in Chapter VIII.

TABLE VI-3

ASSIGNMENT AND POSITIONS OF THE OBSERVED NIR's OF FLUOROBENZENE

Position of Resonance* (eV) π_4	π_5	π_6	Reference	Method
(1.35)§	(1.35)§		Naff et al., (1968)	Scavenger
(1.27)	(1.74)		Christophorou et al., (1974)	TEE#
0.89	not resolved	(4.77)	Jordan et al., (1976)	Transmission
0.82	(1.40)	(4.66)	Present work	Transmission

*Values in parentheses are the energy positions of the maxima of the NIR's.
Values not in parentheses are the energy position of the first vibronic levels of the first NIR.

§Assignment of resonance configuration not made.

#Threshold-electron-excitation.

TABLE VI-4

PERTINENT INFORMATION FOR FLUOROBENZENE

Ionization Energies (eV)			Electron Affinities (eV)			Vibrational Energies (meV)		
						cation	neutral	anion
$(12.5)^{*}_{5}$	$(9.86)_{1}$	$(9.5)_{1}$	$(-1.0)_{3}$	$(-1.74)_{13}$	(-4.77)	65_{5}	100_{10}	113_{8}
$(12.1)6$	$(9.87)_{4}$	9.20_{2}	$(-1.35)_{12}$	$(-1.40)_{8}$	$(-4.66)_{8}$	129_{5}	125_{11}	115_{9}
$(12.3)_{7}$	$(9.82)_{5}$	9.20_{3}	$(-1.27)_{13}$					
	$(9.7)_{6}$	9.21_{4}	-0.89_{9}					
	9.63_{7}	9.11_{5}	-0.82_{8}					
		$(9.3)_{6}$	$(-1.2)_{15}$					
		9.19_{7}	$(-1.40)_{14}$					

*Ionization energies in parentheses are vertical values.
Ionization energies not in parentheses are adiabatic values.

**Values not in parentheses are true electron affinities.
Values in parentheses are vertical attachment energies.

References for Table VI-4 will be found on page 89.

1,4-difluorobenzene

Electron transmission spectra of 1,4-difluorobenzene for incident electron energies from thermal energies to seven electron volts exhibit three distinct structures. The first of these, centered at 0.62 ± 0.06 eV, exhibits pronounced fine structure. The first vibronic level occurs at an incident electron energy of 0.53 ± 0.04 eV. This structure is attributed to NIR formation with the bound electron going into the orbital. The molecule thus has a π-electron affinity of -0.53 ± 0.04 eV and a π-vertical attachment energy of -0.62 ± 0.06 eV.

Interpretation of the fine structure on the lowest NIR of 1,4-difluorobenzene as being due to vibronic levels of the negative ion is consistent with the benzene and fluorobenzene data. We assign the origin of this complicated fine structure in 1,4-difluorobenzene to two overlapping vibrational progressions: the first being slightly anharmonic with a v = 0--v = 1 spacing of 0.110 eV and the second being anharmonic with v = 0--v = 1 spacing of 0.105 eV.

The two remaining structures in the transmission spectra of 1,4-difluorobenzene are broad, symmetric, and without fine structure. They are centered at 1.41 ± 0.06 and 4.51 ± 0.06 eV so that in our present interpretation they correspond to negative ion resonances for electron attachment into the π_5 and π_6 orbitals, respectively. They correspond to vertical attachment energies of -1.41 ± 0.06 eV and -4.51 ± 0.06 eV, respectively.

Table VI-5 is a brief summary of certain information concerning the 1,4-difluorobenzene molecule. This information will be considered in Chapter VIII.

1,3,5-trifluorobenzene

Only two structures are observed in the electron transmission spectra 1,3,5-trifluorobenzene. Both are very symmetric with no visible fine structure. The first is centered at 0.77 ± 0.06 eV and is assigned as the negative ion resonance for electron capture into the degenerate π_4, π_5 orbitals. This degeneracy is a consequence of the molecular symmetry for the 1,3,5-trifluorobenzene molecule and will be discussed in Chapter VIII. The corresponding vertical attachment energy is -0.77 ± 0.06 eV.

The remaining structure is centered at 4.48 ± 0.06 eV and is assigned as the negative ion resonance during which an electron is captured in the π_6 orbital. The vertical attachment energy of this state is thus -4.48 ± 0.06 eV.

A brief summary of information about the 1,3,5-trifluorobenzene positive and negative ions and the neutral molecule is given in Table VI-6.

2,3,5,6-tetrafluorobenzene

The transmission spectra obtained for 2,3,5,6-tetrafluorobenzene exhibit three structural patterns. The first pattern has fine structure which we associate with vibronic levels of the negative ion. The first of these levels occurs for an incident electron energy of 0.34 ± 0.04 eV. The mean

TABLE VI-5

PERTINENT INFORMATION FOR P-DIFLUOROBENZENE

Ionization Energies (eV)			Electron Affinities** (eV)			Vibrational Energies (meV)		
						cation	neutral	anion
12.1_4*	$(10.24)_4$	$(9.50)_4$	-0.53_1	$(-1.41)_1$	$(-4.51)_1$	107_{11}	106_2	110_1
12.16_7	10.04_7	9.15_7	$(-0.6)_6$				104_2	105_1
12.12_8	10.07_8	9.18_8					106_3	
12.18_9	9.98_{10}	9.15_{10}					102_3	
$(12.6)_{12}$	$(10.0)_{12}$	$(9.4)_{12}$						
		9.15_5						
		9.17_6						
		9.21_9						

*Ionization energies in parentheses are vertical values.
Ionization energies not in parentheses are adiabatic values.

**Values not in parentheses are true electron affinities.
Values in parentheses are vertical attachment energies.

List of references for Table VI-5 will be found on page 89.

TABLE VI-6

PERTINENT INFORMATION FOR 1,3,5-TRIFLUOROBENZENE

Ionization Energies* (eV)		Electron Affinities (eV)		Vibrational Energies (meV)		
π_1	π_2, π_3	π_4, π_5	π_6	pos. ion	neutral	neg. ion
12.35_2	9.62_2	$(-0.77)_1$	$(-4.48)_1$	70_4	72_5	***
12.35_4	9.30_3			120_4	125_5	
12.28_6	9.64_4			180_4	167_5	
	9.62_6					

*Ionization energies not in parentheses are adiabatic values.
Ionization energies in parentheses are vertical values.

**Values in parentheses are vertical attachment energies.

***Not observed.

1. Present work
2. Allan and Maier (1975)
3. Brown and Phillips (1974/75)
4. Gilbert, et al. (1972)
5. Nielsen, et al. (1950)
6. Narayan and Murrell (1970)

vibrational spacing is 0.110 eV for the four resolved levels. This structure is assigned to the negative ion resonance for electron capture into a π_4 orbital. The first EA is thus -0.34 ± 0.04 eV. Since the center resonance is at 0.50 ± 0.06 eV we have the first VAE as -0.50 ± 0.06 eV.

The remaining two structures are centered at 1.29 ± 0.06 eV and 4.51 ± 0.06 eV. They are assigned as being due to negative ion resonances with the VAE for the π_5 orbital being -1.29 ± 0.06 eV and the VAE for the π_6 orbital being -4.51 ± 0.06 eV.

Table VI-7 is a summary of information for this molecule.

Pentafluorobenzene

Perhaps more time was spent obtaining electron transmission spectra for pentafluorobenzene (C_6HF_5) than for any other compound studied. The C_6HF_5 compound seemed to cause more disturbance of the experimental apparatus than any other compound we studied. It poisoned the filament more readily than the other compounds studied and seemed to give quite spurious results in general.

The spectrum presented herein for C_6HF_5 exhibits structure which was reproducible over all scans. Other structure was observed from time to time but was not reproducible.

A very sharp structure in the derivative of the transmitted current for C_6HF_5 occurs near the onset of the electron

TABLE VI-7

PERTINENT INFORMATION FOR 2,3,5,6-TETRAFLUOROBENZENE

Ionization Energies* (eV)			Electron Affinities** (eV)			Vibrational Energies (meV)		
π_1	π_2	π_3	π_4	π_5	π_6	pos. ion	neutral	neg. ion
12.35_3	10.04_3	9.36_3	-0.34_6	$(-1.29)_6$	$(-4.51)_6$	93_7	93_1	0.110_6
12.37_5	10.06_5	9.41_5					93_2	
		9.39_4						

*Ionization energies in parentheses are vertical values.
Ionization energies not in parenthese are adiabatic values.

**Values in parentheses are vertical attachment energies.

1. Ferguson, et al. (1953)
2. Green and Harrison (1976)
3. Streets and Ceasar (1973)
4. Bralsford, et al. (1960)
5. Narayan and Murrell (1970)
6. Present work
7. Allan and Maier (1975)

beam (see Figure VI-3). This corresponds to a sharp drop in the current near zero energy which indicates some process which removes electrons from the incident electron beam. The center of this structure is located at approximately 0.4 eV. Assignment of -0.4 eV as the vertical attachment energy corresponding to the π_4 orbital would be only a lower limit of this VAE value. The onset of the beam seems to occur such that we observe only a portion of the resonance structure (viz. that portion corresponding to negative energies). Since we can not measure positive VAE's we must rely on our present results to give us a lower bound on the VAE of the π_4 orbital.

Structure is observed at an electron energy 1.19 ± 0.06 eV. We interpret this to be due to the NIR associated with the π_5 orbital. The corresponding VAE is -1.19 ± 0.06 eV.

The remaining structure on the electron transmission spectrum for pentafluorobenzene is centered at 4.53 ± 0.06 eV. This is assigned as the π_6 capture with a VAE of -4.53 ± 0.06 eV.

Table VI-8 is a summary of information about pentafluorobenzene similar to those tables already presented for the other fluorobenzenes.

Hexafluorobenzene

To complete the series of fluorobenzenes we consider the electron transmission spectrum of hexafluorobenzene (C_6F_6). Two broad, featureless structures are observed in

TABLE VI-8

PERTINENT INFORMATION FOR PENTAFLUOROBENZENE

Ionization Energies (eV)			Electron Affinities (eV)			Vibrational Energies (meV)		
π_1	π_2	π_3	π_4	π_5	π_6	pos. ion	neutral	neg. ion
12.50_2	$10.2_{2,3}$	9.64_2	$\sim 0._6$	$(-1.19)_8$	$(-4.53)_8$	89_3	89_1	***
12.47_7	9.73_7	$9.84_{4,5}$	$\sim 0._8$					
		9.8						
		9.55_7						

*Ionization energies in parentheses are vertical values.
Ionization energies not in parentheses are adiabatic values.

**Values in parentheses are vertical attachment energies.

***Not observed.

1. Steele and Whiffen (1960)
2. Streets and Ceasar (1973)
3. Allan and Maier (1975)
4. Bralsford, et al. (1960)
5. Brown and Phillips (1974/75)
6. Naff, et al. (1968)
7. Narayan and Murrell (1970)
8. Present work

the transmission spectrum for C_6F_6. The first is centered at 0.42 ± 0.06 eV and the second at 4.50 ± 0.06 eV.

Both structures are assigned as NIR's with the first associated with the π_4, π_5 degenerate orbitals and the second associated with the π_6 orbital. The vertical attachment energies are thus -0.42 ± 0.06 eV and -4.50 ± 0.06 eV, respectively.

Considering the transmission spectrum of C_6F_6 in detail we note a small structure preceding the broader resonance structure. This is common to all transmission spectra obtained for all fluorobenzenes. It occurred in approximately the same location on every scan. It could possibly be an instrumental effect caused as the sample gas interferes with the beam monochromator region (see Chapter IV).

To insure that this small structure was not a vibrational level of the C_6F_6 negative ion, I obtained spectra which were not of the derivative of the transmitted current, but rather of the actual transmitted current versus incident electron energy. Figure VI-5 shows such a spectrum for N_2, C_6H_6, and C_6F_6. The structure in each has the same form indicating a NIR in each case. The onset of the resonant structure is well separated from the onset of the beam signifying that we are seeing the entire resonance and not just the upper portion of the resonance.

The summary of information concerning the hexafluorobenzene molecule is found in Table VI-9. This material will be discussed in some detail in Chapter VIII.

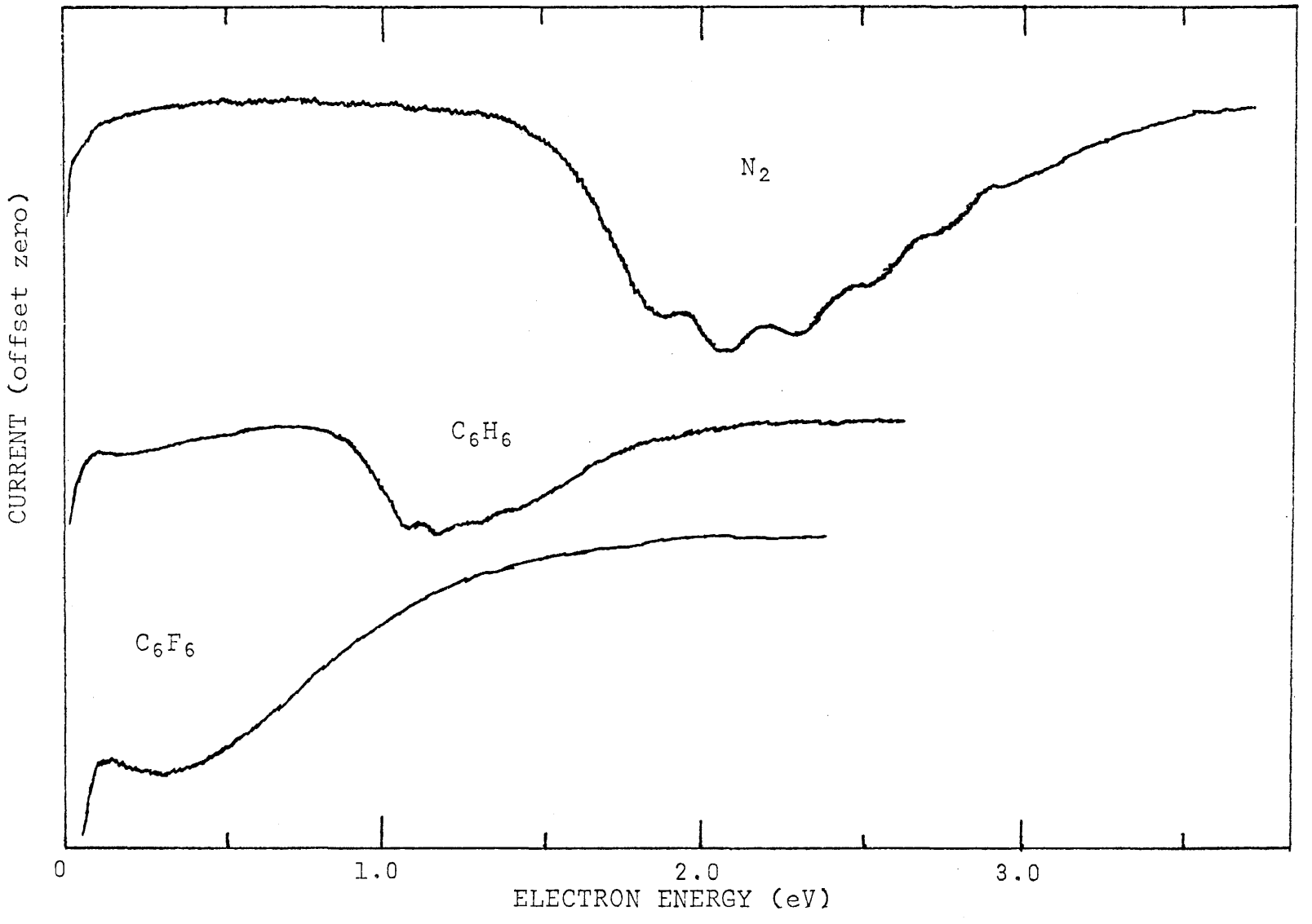

Figure VI-5. Electron transmission spectra for N_2, C_6H_6, and C_6F_6.

TABLE VI-9

PERTINENT INFORMATION FOR HEXAFLUOROBENZENE

Ionization Energies* (eV)		Electron Affinities** (eV)		Vibrational Energies (meV)		
π_1	π_2, π_3	π_4, π_5	π_6	pos. ion	neutral	neg. ion
$12.58_{4,7}$	9.97_3	$+1.8_9$	(-0.73)	50_4	$69_{1,2}$	***
$(12.77)_4$	$9.93_{4,7}$	$(-0.42)_{11}$	$(-4.50)_{11}$	180_4	55_1	
12.56_8	$(10.12)_4$	$+1.20_{12}$		66_4		
11.12_5	9.88_5			67_6		
11.64_5	9.90_8			189_6		
12.71_5	9.					

*Ionization energies in parentheses are vertical values.
Ionization energies not in parentheses are adiabatic values.

**Values in parentheses are vertical attachment energies.

***Not observed.

List of references for Table VI-9 will be found on page 89.

List of references for TABLE VI-4.

1. Baker, et al. (1968)
2. Bralsford, et al. (1960)
3. Brown and Phillips (1974/75)
4. Clark and Frost (1967)
5. Debies and Rabalais (1972/73)
6. Klessinger (1972)
7. Streets and Ceasar (1973)
8. Present work
9. Jordan, et al. (1976)
10. Smith, et al. (1953)
11. Clark and McCaffery (1977)
12. Naff, et al. (1968)
13. Christophorou, et al. (1974)
14. Hadjiantoniou, et al. (1973)
15. Compton, et al. (1966)

List of references for TABLE VI-5.

1. Present work
2. Ferguson, et al. (1953a)
3. Guttman and Rice (1974)
4. Baker et al. (1968).
5. Bralsford et al. (1960)
6. Brown and Phillips (1974/75)
7. Clark and Frost (1967)
8. Gilbert and Sandorfy (1974)
9. Narayan and Murrell (1970)
10. Streets and Ceasar (1977)
11. Duke, et al. (1977)
12. VonNiessen, et al. (1977)

List of references for TABLE VI-9.

1. Steele (1962)
2. Delbouille (1956)
3. Brown and Phillips (1974/75)
4. Brundle, et al. (1972)
5. Clark and Frost (1967)
6. Duke, et al. (1977)
7. Narayan and Murrell (1970)
8. Streets and Ceasar (1973)
9. Lifshitz, et al. (1973)
10. Gant and Christophorou (1976)
11. Present work
12. Chen and Wentworth (1975)

CHAPTER VII

NEGATIVE ION RESONANCES OF BIPHENYL

I. INTRODUCTION

Biphenyl is an interesting molecule in many respects. Physically it is of importance as the simplest singly-bonded polycyclic aromatic hydrocarbon. The bond strength and orientation between the two phenyl groups are fundamentally important quantities.

Recently, the danger of multiply halogenated biphenyls in our environment has been recognized (see, e.g. Kay, 1977). Many biphenyl compounds are thought to be carcinogenic (Kay, 1977, and references therein).

Measurement of the basic properties of biphenyl is necessary before a comprehensive theory of molecular reaction processes can be reached. In this chapter we consider the measurement of the vertical attachment energies of biphenyl in the vapor phase.

II. EXPERIMENTAL RESULTS

At room temperature (25°C) biphenyl is a white solid compound with a noticeable odor. The vapor pressure at 25°C is approximately $8. \times 10^{-3}$ torr. The sample used in the present experiment was obtained from James Hinton, Newport News, Virginia, with a stated minimum purity of 99.999%, so that further purification was deemed unnecessary. Submitting

the sample for a short time to a high vacuum system was performed to remove gases from the sample container. No other degassing process was performed.

The unheated solid sample yielded insufficient vapor pressure in the collision chamber. The manifold and inlet tube were then heated with conventional heater tapes while a hot water (55°C) bath was placed around the sample container. This increased the vapor pressure in the collision chamber to a level such that approximately 20% of the incident electron beam was removed from the transmitted current.

An electron transmission spectrum for biphenyl in the vapor phase is presented in Figure VII-1. Instrumental resolution for this compound is inferior to that previously obtained for either benzene or the fluorobenzenes. This is most likely due to attachment of biphenyl to surfaces of the electron monochromator and other components since the TEM was not specially heated other than through the heat provided by the radiant heating from the solenoid.

There are three obvious structures in the derivative of the transmitted current of biphenyl for incident electron energies from thermal to 3.0 eV. The first structure is centered at 0.44 ± 0.06 eV with faintly visible fine structure. This fine structure was observed in all scans but cannot be resolved more clearly. This structure is assigned to be a negative ion resonance with a corresponding VAE of -0.44 ± 0.06 eV.

A structure broader than that of any observed single

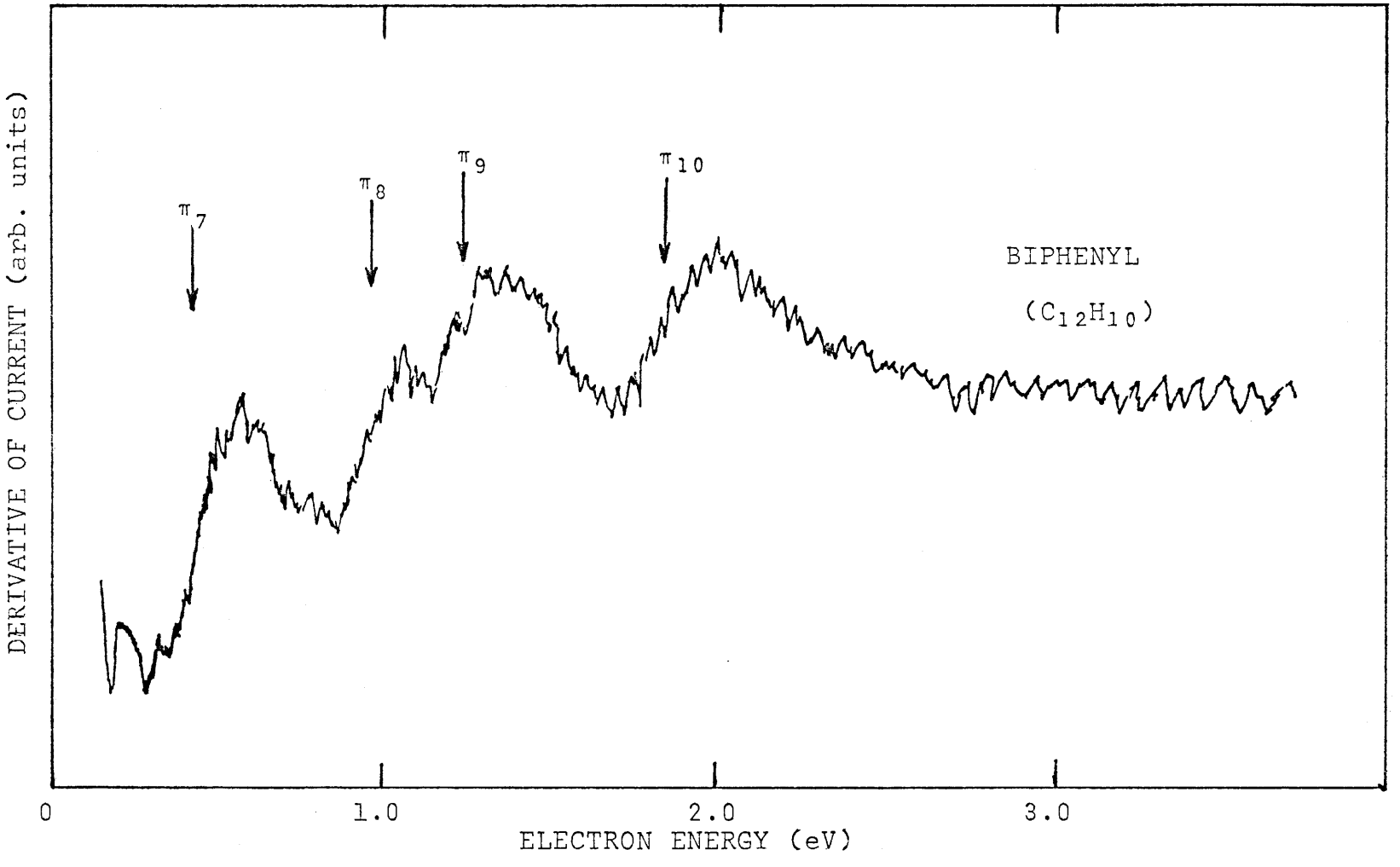

Figure VII-1. Electron transmission spectrum of biphenyl.

NIR is found to be centered at 1.11 ± 0.06 eV. The characteristics of this are not those of vibrational structure previously observed. The width of this structure is very nearly twice the width of any previously observed single NIR. We could therefore approximate this structure as being two NIR's centered at 0.93 ± 0.08 eV and 1.27 ± 0.08 eV. The corresponding vertical attachment energies are -0.93 ± 0.08 eV and -1.27 ± 0.08 eV.

The remaining observed structure in the biphenyl spectrum is centered at an incident electron energy of 1.88 ± 0.06 eV. The vertical attachment energy is therefore -1.88 ± 0.06 eV.

III. DISCUSSION OF RESULTS

In the vapor phase the biphenyl molecule is nonplanar The dihedral angle (angle between the planes of the two phenyl rings) has been found by electron diffraction experiments to be approximately 42° in the vapor phase (Almenningen and Bastiansen, 1958).

The biphenyl molecule is basically two benzene rings joined by a single carbon-carbon bond. There are three filled π-orbitals for each benzene ring making a total of six filled π-orbitals for biphenyl. We shall call these π_1, π_2, π_3, π_4, π_5, and π_6 (being careful that we not confuse the present π_4, π_5, and π_6 orbitals with the unfilled π-orbitals of each benzene ring). The unfilled orbitals of biphenyl are thus denoted as π_7, π_8, π_9, π_{10}, π_{11}, and π_{12}.

A NIR can occur by capture of an additional electron into one of the unfilled π-orbitals. We assign the lowest energy NIR of biphenyl as being due to electron capture into the π_7 orbital. The NIR next higher in energy would correspond to electron capture into the π_8 orbital, and so forth.

Each benzene ring has its own π-electron structure of the same symmetry. We thus expect a large π-π interaction between the energy levels of the π_4, π_5 degenerate orbitals of each benzene ring to yield the observed energy levels of biphenyl. Our present experimental results seem to confirm this. For a planar molecular geometry we would expect no π_5-π_5 interaction between the rings. But since biphenyl is nonplanar in the vapor phase we expect that some π_5-π_5 interaction may be present. The π_4-π_4 interaction is expected to be large due to the symmetry of each phenyl ring. Vertical attachment energies for benzene and biphenyl are shown in Figure VII-2. The lines connecting the benzene VAE's with the VAE's of biphenyl serve as an indication of the consequences of the π-π interaction between the two benzene rings.

IV. SUMMARY

Although only a narrow energy range is considered for incident electron energies, the energy range is sufficient to illustrate the ring-ring interactions of the biphenyl molecule. The addition of the biphenyl data to that of the fluorobenzenes in this work serves to indicate areas of application of the present experimental technique.

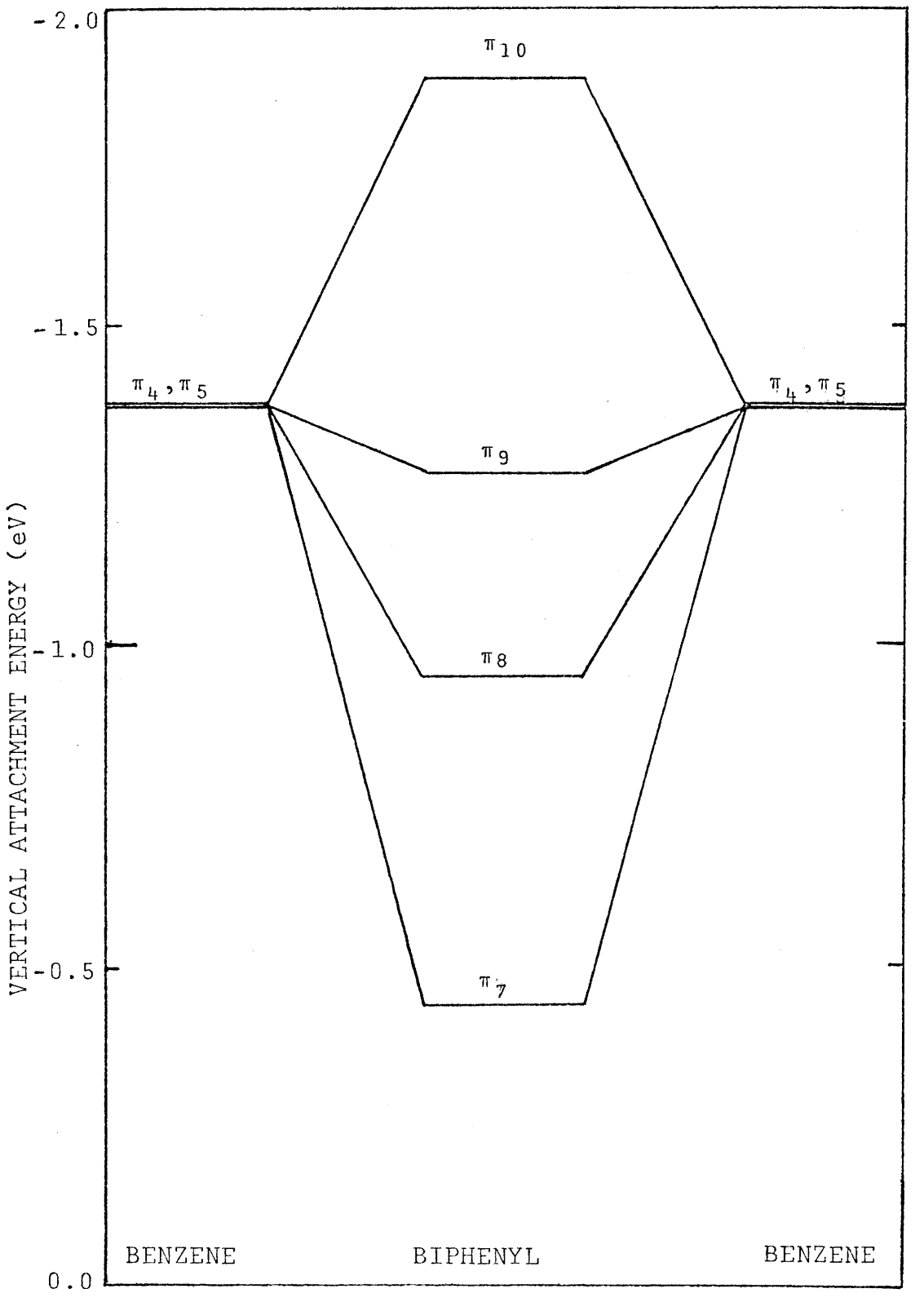

Figure VII-2. VAE's of benzene and biphenyl showing the effects of the π-π interactions.

Solid samples need to be treated in a more careful manner so that instrumental resolution can be improved. An extended energy scan would likely show the π_6-π_6 interactions of the two benzene rings in the biphenyl molecule.

CHAPTER VIII

SUMMARY AND CONCLUDING REMARKS

I. SYMMETRY CONSIDERATIONS

The molecules considered in Chapter V and Chapter VI (viz. benzene and fluorobenzenes) are of symmetry point groups as follows: benzene, D_{6h}; fluorobenzene, C_{2v}; 1,4-difluorobenzene, D_{2h}; 1,3,5-trifluorobenzene, D_{3h}; 2,3,5,6-tetrafluorobenzene, D_{2h}; pentafluorobenzene C_{2v}; and hexafluorobenzene, D_{6h}. We thus have a group of molecules which form a continuous series of symmetry point groups. Comparison of the experimental results for fluorine substitution onto benzene with results for hydrogen "substitution" onto hexafluorobenzene can yield important information about the so called "substituent effects" on substituted benzene.

II. INDUCTIVE EFFECT

As previously stated (Chapter V) the lowest shape resonance of benzene is attributed to the temporary capture of a low-energy electron into the degenerate e_{2u} (symmetric and antisymmetric) states of the benzene molecule. The corresponding molecular orbitals are π_4 and π_5, for $e_{2u,s}$ and $e_{2u,a}$, respectively. These are the two lowest unfilled π orbitals of the ground state of the neutral molecule. Analysis of the inelastically scattered electrons indicate that this is f-wave ($\ell = 3$) partial wave scattering (Wong and Schulz, 1975).

The introduction of a substituent upon the benzene ring destroys the D_{6h} symmetry of the benzene molecule and thereby removes the degeneracy of the lowest unfilled orbitals. In addition to the presentation of the initial detection of the double shape resonances in fluorobenzene, Christophorou, et al. (1974) set forth a first-order-perturbation-theory calculation to account for the observed splitting of the orbital energies. We now extend that treatment to include π_4, π_5 splitting of multiply substituted benzene derivatives (namely, the fluorobenzenes with one to six substituents). We also consider the effect of fluorine substitution on the π_6 orbitals.

Perturbation of the π orbitals of the benzene molecule following substitution by an atom or a group of atoms onto the benzene ring depends strongly upon the resonance and inductive properties of the substituent(s). The resonance effect is caused by the interaction of substituent orbitals of suitable symmetry with the π orbitals of the benzene ring which, in turn, leads to charge transfer either to or from the substituent. The inductive effect is due to changes in the electronegativity of the carbon atom to which the substituent is attached and/or repulsion between the aromatic π electrons and substituent p-electrons (Baker et al., 1968). The net result of the inductive effect is the transfer of electron charge density to or from the ring. A strongly electronegative substituent, such as fluorine, causes a redistribution of the π electron density from the benzene

ring to the fluorine atom (inductive effect).

We assume in the present calculations that the geometry of the molecule is unchanged upon fluorine substitution and upon electron attachment. The positions of the six carbon atoms are shown on page 68. Introduction of a fluorine atom onto the (1) position (to form fluorobenzene) would cause a change in the net π electron density of the benzene ring. We consider the following mathematical description of the substituent effect on the orbital energies based upon LCAO (Linear Combination of Atomic Orbitals) theory.

If we define $\delta\varepsilon_\rho^{(1)}$ as the first order energy correction when a perturbation δV is applied to the molecule whose zeroth order wave function is ψ_ρ^o we have

$$\delta\varepsilon_\rho^{(1)} = \int \overline{\psi_\rho^o}\ \delta V\ \psi_\rho^o\ dx^3 \qquad \text{VIII-1}$$

where the subscript ρ indicates the π-molecular orbital to which the wave function corresponds.

For the benzene molecule we may write the wave function as

$$\psi_\rho^o = \sum_{\nu=1}^{6} C_{\rho\nu}\ \phi_{p_z}(\vec{r}-\vec{R}_\nu) \qquad \text{VIII-2}$$

where $\phi_{p_z}(\vec{r}-\vec{R}_\nu)$ is the wave function of the p-orbital of the ν th carbon atom. (Note that we are concerned only with the p_z or π wave function.)

The coefficients $C_{\rho\nu}$ are found by normalization of the wave function. The values $C_{\rho\nu}$ are shown in Figure VIII-1, where $\rho = 4, 5$, or 6 corresponding to the π_4, π_5, or π_6 orbitals,

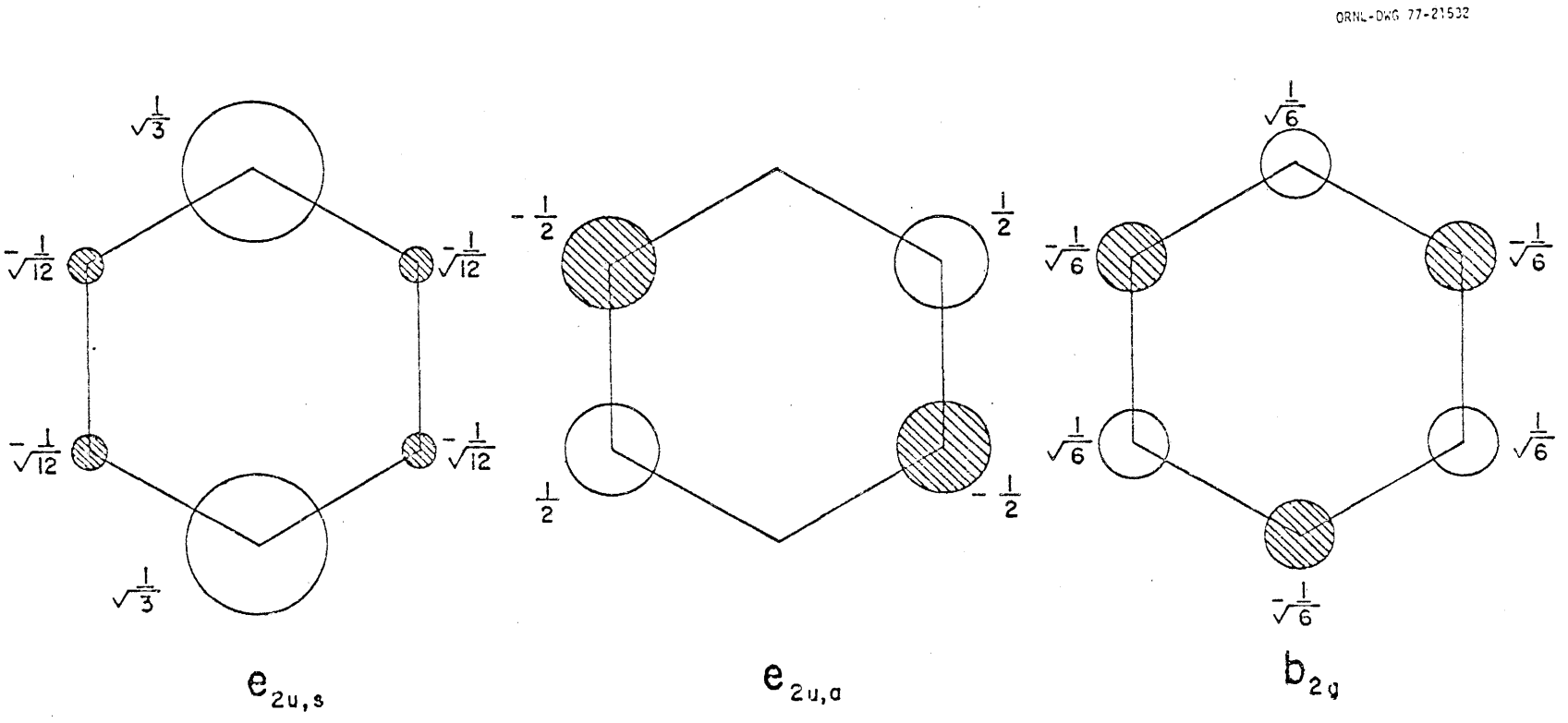

Figure VIII-1. Unfilled π orbitals of benzene showing the coefficients of the atomic orbitals of the carbon atoms.

respectively,

Using Equation VIII-2 in Equation VIII-1 we have

$$\delta\varepsilon_\rho^{(1)} = \int \sum_{\nu=1}^{6} \overline{\phi_{p_z}(\vec{r}-\vec{R}_{\nu'})}\,\overline{C_{\rho\nu'}}\,\delta V \sum_{\nu=1}^{6} C_{\rho\nu}\phi_{p_z}(\vec{r}-\vec{R}_\nu)\,dx^3 \qquad \text{VIII-3}$$

$$\text{or } \delta\varepsilon_\rho{}^1 = \sum_{\nu'}\sum_{\nu} \overline{C}_{\rho\nu'} C_{\rho\nu} \int \overline{\phi_{p_z}(\vec{r}-\vec{R}_{\nu'})}\,\delta V \phi_{p_z}(\vec{r}-\vec{R}_\nu)\,dx^3 \quad . \qquad \text{VIII-4}$$

If we let γ = constant = δV for each substituent position ν and neglect any overlap of the wave functions we have

$$\delta\varepsilon_\rho^{(1)} = \gamma \sum_{\nu} |C_{\rho\nu}|^2 \quad . \qquad \text{VIII-5}$$

The magnitude of $\delta\varepsilon_\rho{}^1$ for any fluorinated benzene for the ρ th orbital is then found by applying Equation VIII-5. As an example, the shift in the energy level of the π_4 orbital (e_{2u}) of 1,3,5-trifluorobenzene is

$$\delta\varepsilon_4^{(1)} = \gamma \left[\left(\frac{1}{\sqrt{3}}\right)^2 + \left(\frac{-1}{\sqrt{12}}\right)^2 + \left(\frac{-1}{\sqrt{12}}\right)^2 \right] = \tfrac{1}{2}\gamma$$

In the same manner perturbations of the π_4, π_5, and π_6 orbital energies for the present series of fluorobenzenes are calculated. These results are shown in Table VIII-1.

The difference in the orbital energy of a π orbital of benzene with the energy of the same π orbital of one of the fluorobenzenes should be equal to the difference in corresponding vertical attachment energies of the benzene molecule and the fluorobenzene molecule considered. Figure VIII-2 illustrates the experimentally determined vertical attachment energies (solid lines) for benzene and the

TABLE VIII-1

CALCULATION OF ENERGY SHIFTS

Position of Fluorine Substituent	π_4 energy shift	π_5 energy shift	π_6 energy shift
1	1/3 γ	0	1/6 γ_1*
1,4	2/3 γ	0	1/3 γ_1
1,3,5	1/2 γ	1/2 γ	1/2 γ_1
2,3,5,6	1/3 γ	γ	2/3 γ_1
2,3,4,5,6	2/3 γ	γ	5/6 γ_1
1,2,3,4,5,6	γ	γ	γ_1

*Since there is no reason to assume that γ for the π_4 and π_5 orbitals should be the same as γ for the π_6 orbitals, we therefore refer to the latter as γ_1.

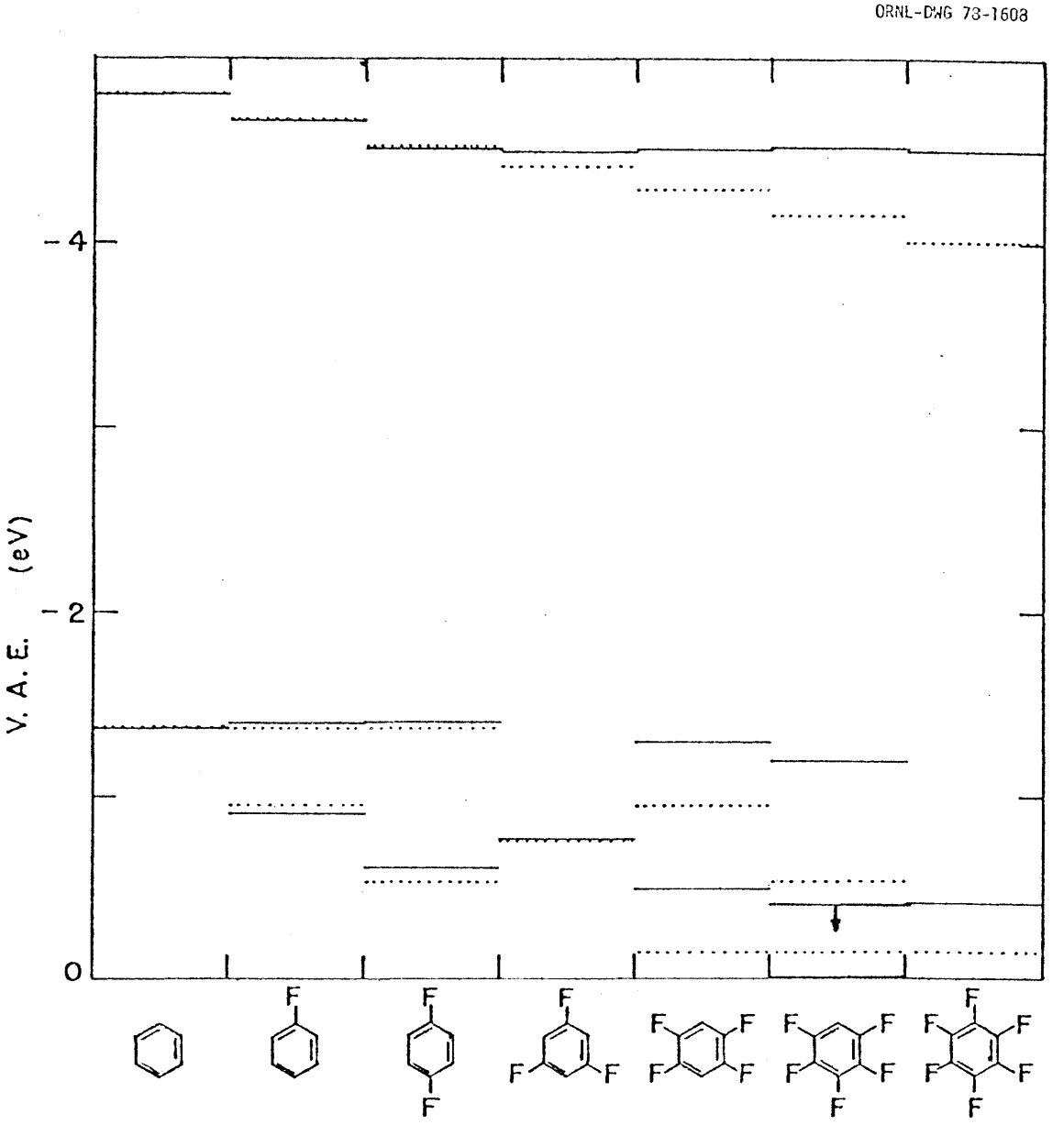

Figure VIII-2. Comparison of experimental values (——) and theoretical values (····) of the VAE's for benzene and the fluorobenzenes.

fluorobenzenes. The dotted lines are based on the theoretical values of Table VIII-1 where we fit the first four VAE energy differences to obtain γ = 1.24 eV and γ_1 = 0.78 eV.

Experimental values and theoretical values of Figure VIII-2 agree very well for benzene, fluorobenzene, 1,4-difluorobenzene and 1,3,5-trifluorobenzene. The difference between theory and experiment become large for 2,3,5,6-tetrafluorobenzene, pentafluorobenzene, and hexafluorobenzene. This is expected since only first order effects are calculated with no consideration for "nearest neighbor" effects of adjacent fluorine atoms. From the experimental results fluorine-fluorine interactions appear to be important since increased deviations between theory and experiment exist as the number of fluorine atoms increases.

III. ASSIGNMENT OF THE π_4, π_5 NIR IN HEXAFLUOROBENZENE

Hexafluorobenzene is known to have a positive electron affinity (Lifshitz et al., 1973) which is 1.8 ± 0.3 eV. Gant and Christophorou (1976) first detected the NIR at 0.73 eV and made the assignment of this resonance as being electron capture into the π_6 orbital.

A systematic progression of the experimental vertical attachment energies for the series of fluorobenzenes is shown in Figure VIII-2. Assignment of π_6 orbitals as corresponding to the uppermost series of vertical attachment energies is consistent throughout the entire series. This is to say that the -4.50 eV VAE of hexafluorobenzene

corresponds to capture into the π_6 orbital.

The same trend is observed for the π_4, and π_5 orbital assignments indicating that the -0.42 eV VAE of hexafluorobenzene corresponds to electron capture into the degenerate π_4, π_5 orbitals. The remaining question is: What is the source of the + 1.8 eV EA of hexafluorobenzene?

Yim and Wood (1976) identified the negative ion state of hexafluorobenzene as belonging to a planar σ^*-radical. From electron spin resonance studies Symons et al. (1977) assigned the $C_6F_6^-$ structure as a puckered-ring structure with a σ or a pseudo π delocalization. Both of these studies contradict the assignment made by Gant and Christophorou (1976).

Vertical ionization potentials (Narayan and Murrell, 1970) and experimental vertical attachment energies are shown in Figure VIII-3. Note the trends in each case that the π-orbitals become more stabilized upon fluorine substitution although differences between orbital energies for C_6H_6 and C_6F never exceed 1.00 eV. Observation of this trend was made by Brundle et al. (1972) for the π ionization potentials. In that work the authors set forth the "perfluoro effect" for ionization potentials of aromatic molecules. In addition to the slight increase in stability of the π electron orbitals there is a large increase (several volts) in the σ-ionization potentials when going from the perhydro compound to the perfluoro compounds.

If a similar "perfluoro effect" exists for negative

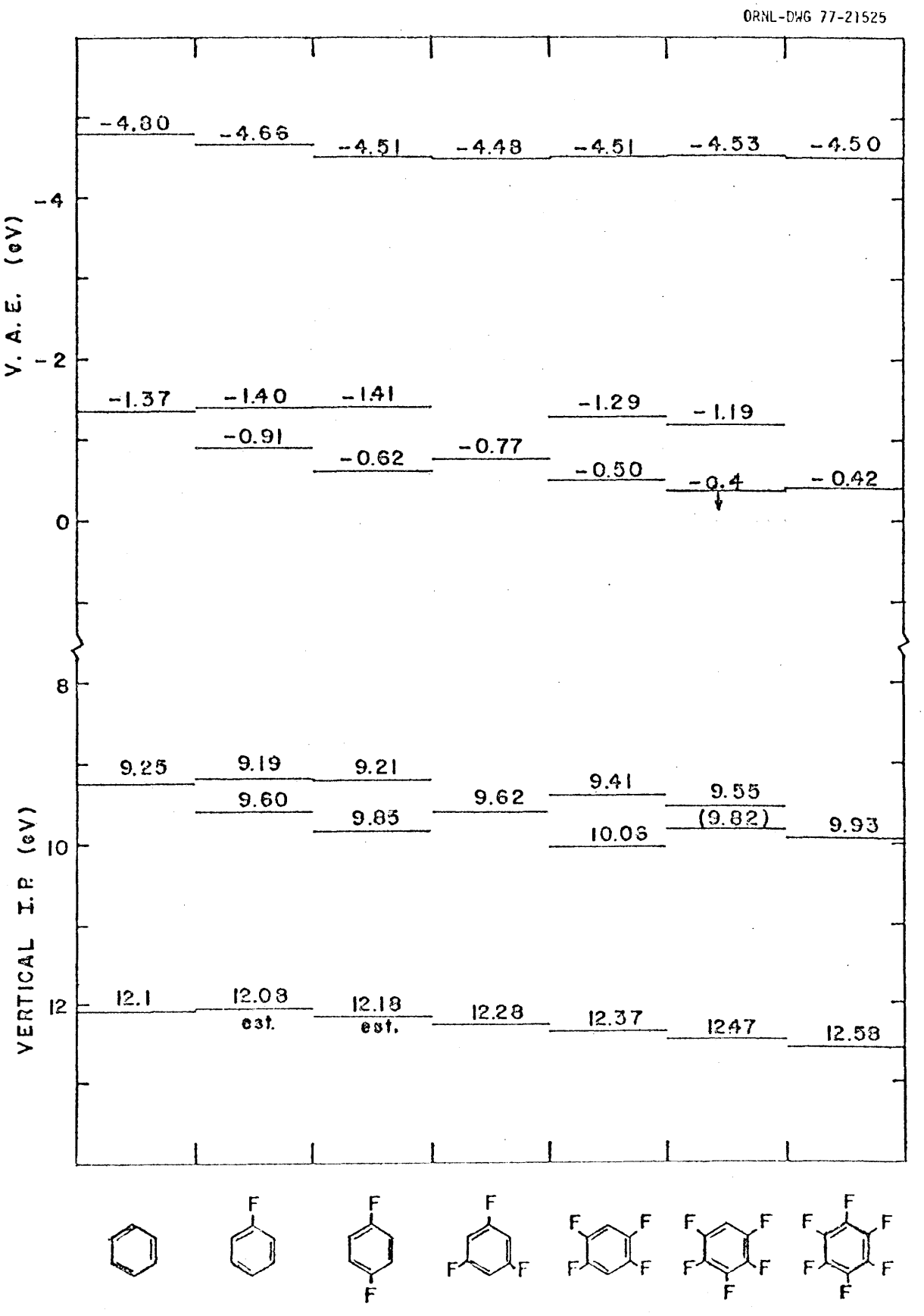

Figure VIII-3. VAE's and IP's for Benzene and Fluorobenzene.

ion states then the positive EA of C_6F_6 could be σ-orbital electron attachment. This would indicate that a σ-orbital resonance is the lowest lying resonance of C_6F_6. The ∿0.0 eV electron attachment resonance observed by Gant and Christophorou (1976) could then be assigned to such a NIR.

IV. CONCLUDING REMARKS

In the present work a new experimental device was built, tested, and applied to the study of NIR's of a basic series of organic molecules. The importance of this work is threefold:

1. It has demonstrated that such a device can yield accurate values of electron affinities and vertical attachment energies.
2. A complete series of fluorine-substituted benzene derivatives has been studied to yield their electron affinities and/or vertical attachment energies. This has provided new insights concerning the negative ion states of these molecules.
3. Solid samples (with sufficient vapor pressures) can be studied with the present device to measure their VAE's and/or EA's. Such a sample is biphenyl for which VAE's were measured which, in turn, yielded information of the interaction of the two benzene rings.

Although negative ion resonances of benzene and the fluorobenzenes exist for very short lifetimes in isolated molecule conditions (i.e. the present work), their existence in condensed systems (eg. biosystems) is of fundamental importance in radiation damage. During low-energy electron interactions, these molecules can undergo inelastic resonance scattering whereby the molecule is left in a vibrationally excited state. The lifetime of this state can be sufficiently long to allow for chemical (biochemical) reactions.

LIST OF REFERENCES

LIST OF REFERENCES

Abouaf, R., R. Paineau, and F. Fiquet-Fayard, J. Phys. B 9, 303 (1976).

Allan, M., and J. P. Maier, Chem. Phys. Lett. 34, 442 (1975).

Almenningen, A., and O. Bastiansen, Kgl. Norske Videnskab. Selakabs. Skrifter 4, 1 (1958).

Asbrink, L., E. Lindholm, and O. Edquist, Chem. Phys. Lett. 5, 609 (1970).

Bailey, L. E., Rev. Sci. Instrum. 31, 1147 (1960).

Baker, A. D. , D. P. May, and D. W. Turner, J. Chem. Soc. (B) 1968, 22 (1968).

Bardsley, J. N., and F. Mandl, Rep. Prog. Phys. 31, 472 (1968).

Barr, W. L., and W. A. Perkins, Rev. Sci. Instrum. 37 1354 (1966).

Barrett, R. M., and D. Steele, J. Mol. Structure 11, 105 (1972).

Bates, D. R., Atomic and Molecular Processes, Academic Press, New York, 1962.

Bleakney, W., and J. A. Hipple, Jr., Phys. Rev. 53, 521 (1938).

Boness, M. J. W., I. W. Larkin, J. B. Hasted, and L. Moore, Chem. Phys. Lett. 1, 292 (1967).

Bralsford, R., P. V. Harris, and W. C. Price, Proc. Roy. Soc. A258, 459 (1960).

Brown, R. G., and D. Phillips, J. Photochem. 3, 337 (1974/75).

Brundle, C. R., M. B. Robin, N. A. Kuebler, J. Am. Chem. Soc. 94, 1466 (1972).

Burke, P. G., Potential Scattering in Atomic Physics, Plenum Press, New York, 1977.

Burrow, P. D., J. A. Michejda, and K. D. Jordan, J. Am. Chem. Soc. 98, 6392 (1976).

Chen, E. C. M., and W. E. Wentworth, J. Chem. Phys. 63, 3183 (1975).

Christophorou, L. G., Atomic and Molecular Radiation Physics, John Wiley and Sons, New York, 1971.

Christophorou, L. G., Photochemistry and Photobiology, (In Press) (1977).

Christophorou, L. G., and R. N. Compton, Health Physics 13, 1277 (1967).

Christophorou, L. G., M. W. Gant, and D. L. McCorkle, Advances in Chemical Physics Vol. XXXVI, I. Prizogine and S. A. Rice (Eds.), John Wiley and Sons, New York, 1977, pp. 413-520.

Christophorou, L. G., D. L. McCorkle, and J. G. Carter, J. Chem. Phys. 60, 3779 (1974).

Clark, I. D., and D. C. Frost, J. Am. Chem. Soc. 89, 244 (1967).

Clark, R., and A. J. McCaffery, J. Phys. Chem. 81, 1918 (1977).

Compton, R. N., L. G. Christophorou, and R. H. Huebner, Phys. Lett. 23, 656 (1966).

Curran R. K., J. Chem Phys. 38, 780 (1963).

Dance, D. F., and I. C. Walker, Proc. Roy. Soc. (London) A334 , 259 (1973).

Debies, T. P., and J. W. Rabalais, J. El. Spectros. 1, 355 (1972/73).

Delbouille, L., J. Chem. Phys. 25, 182 (1956).

Dewar, M. J. S., E. Haselbach, and S. D. Worley, Proc. Roy. Soc. (London) A315, 431 (1970).

Duke, C. B., and N. O. Lipari, Chem. Phys. Lett. 36, 51 (1975).

Duke, C. B., K. L. Yip, G. P. Ceasar, A. W. Potts, and D. G. Streets, J. Am. Chem. Soc. 66, 256 (1977).

Ehrhardt, H., and K. Willmann, Z. Phys. 204, 462 (1967).

Eland, J. H. D., Int. J. Mass Spectr. Ion. Phys. 2, 471 (1969).

Ferguson, E. E., R. L. Hudson, J. R. Nielsen, and D. C. Smith, J. Chem. Phys. 21, 1464 (1953).

Fesenko, E. P., and L. V. Iogansen, Chem. Phys. Lett. 48, 22 (1977).

Fox, R. E., W. M. Hickam, D. J. Grove, and T. Kjeldaas, Jr., Rev. Sci. Instrum. 26, 1101 (1955).

Gant, K. S., and L. G. Christophorou, J. Chem. Phys. 65, 2977 (1976).

Gilbert, R., and C. Sandorfy, Chem. Phys. Lett. 27, 457 (1974).

Gilbert, R., P. Sauvageau, and C. Sandorfy, Chem. Phys. Lett. 17, 465 (1972).

Golden, D. E., Rev. Sci. Instrum. 44, 1339 (1973).

Green, J. H. S., and D. J. Harrison, Spectrochemica Acta, 32A, 1185 (1976).

Guttman, C., and S. A. Rice, J. Chem. Phys. 61, 661 (1974).

Hadjiantoniou, A., L. G. Christophorou, and J. G. Carter, J. Chem. Soc. Faraday Trans. II 69, 1691 (1973).

Hanley, T. E., J. Appl. Phys. 19, 583 (1948).

Hasted, J. R., Physics of Atomic Collisions, Butterworth, London, 1964.

Herzberg, G., Infrared and Raman Spectra, Van Nostrand, New York, 1945.

Herzberg, G., Electronic Spectra of Polyatomic Molecules, Van Nostrand, New York, 1966.

Herzenberg, A., and F. Mandl, Proc. Roy. Soc. (London) A270, 48 (1962).

Holloway, P. H., and J. B. Hudson, Rev. Sci. Instrum. 43, 828, (1972).

Hubin-Franskin, M. J., and J. E. Collin, Int. J. Mass Spect. Ion Phys. 5, 95 (1972).

Hughes, A. L., and V. Rojansky, Phys. Rev. 34, 284 (1929).

Hush, N. S., and J. A. Pople, Far. Soc. Trans. (London) 51, 600 (1955).

Jordan, K. D., J. A. Michejda, and P. D. Burrow, J. Am. Chem. Soc. 98, 7189 (1976).

Kay, K., Environ. Res. 13, 74 (1977).

Klessinger, M., Angew. Chem. 84, 544 (1972).

Kurepa, M. V., I. M. Cadez, and V. M. Pejcev, Fizika 6, 185 (1974).

Kurepa, M. V., V. M. Pejcev, and I. M. Cadez, J. Phys. D 9, 481 (1976).

Kuyatt, C. E., Methods Exp. Phys. 7A, 1 (1968).

Kuyatt, C. E., S. R. Mielczarek, and J. A. Simpson, Phys. Rev. Lett. 12, 293 (1964).

Kuyatt, C. E., and J. A. Simpson, Rev. Sci. Instrum. 38, 103 (1967).

Kuyatt, C. E., J. A. Simpson, and S. R. Mielczarek, Phys. Rev. 138, A385 (1965).

Larkin, I. W., and J. B. Hasted, J. Phys. B: Atom. Molec. Phys. 5, 95 (1972).

Lifshitz, C., T. O. Tiernan, and B. M. Hughes, J. Chem. Phys. 59, 3182 (1973).

Maier, J. P., and D. W. Turner, Disc. Faraday Soc. 54, 149 (1972).

Marmet, P., and L. Kerwin, Can. J. Phys. 38, 787 (1960).

Massey, H. S. W., Negative Ions, 2nd Ed., Cambridge University Press, Cambridge, 1950.

Massey, H. S. W., Negative Ions, 3rd Ed., Cambridge University Press, Cambridge, 1976.

Massey, H. S. W., and E. H. S. Burhop, Electronic and Ionic Impact Phenomena, Vol. I, Oxford, London, 1969.

Mathur, D., and J. B. Hasted, J. Phys. B: Atom. Molec. Phys. 9, L31 (1976).

McDaniel, E. W., Collision Phenomena in Ionized Gases, John Wiley and Sons, New York, 1964.

Meyer, V. D., A. Skerbele, and E. W. Lassettre, J. Chem. Phys. 43, 805 (1965).

Naff, W. T., C. D. Cooper, and R. N. Compton, J. Chem Phys. 49, 2784 (1968).

Narayan, B., and J. N. Murrell, Mol. Phys. 19, 169 (1970).

Nenner, I., and G. J. Schulz, J. Chem. Phys. 62, 1747 (1975).

Nicolaides, C. A., Phys. Rev. A 6, 2078 (1972).

Nielsen, J.R., C. Liang, and D. C. Smith, Disc. Faraday Soc. 9, 177 (1950).

Pisanias, M. N., Thesis, University of Tennessee, Knoxville (1972).

Roy, D., Rev. Sci. Instrum. 43, 535 (1972).

Sanche, L., and G. J. Schulz, Phys. Rev. Lett. 26, 943 (1971).

Sanche, L., and G. J. Schulz, Phys. Rev. A 5, 1672 (1972).

Sanche, L., and G. J. Schulz, Phys. Rev. A 6, 69 (1972).

Sanche, L., and G. J. Schulz, J. Chem. Phys. 58, 479 (1973).

Schulz, G. J., Phys. Rev. 112, 150 (1958).

Schulz, G. J., Phys. Rev. 136, A650 (1964).

Schulz, G. J., Rev. Mod. Phys. 45, 378 (1973).

Simpson, J. A., Rev. Sci. Instrum. 32, 1283 (1961).

Simpson, J. A., Rev. Sci. Instrum. 35, 1698 (1964).

Simpson, J. A., and U. Fano, Phys. Rev. Lett. 11, 158 (1963).

Smith, D. C., E. E. Ferguson, R. L. Hudson, and J. R. Nielsen, J. Chem. Phys. 21, 1475 (1953).

Spence, D., Phys. Rev. A 10, 1045 (1974).

Spence, D., Phys. Rev. A 11, 1539 (1975).

Spence, D., Phys. Rev. A 12, 721 (1975).

Spence, D., and W. A. Chupka, Phys. Rev. A 10, 71 (1974).

Stamatovic, A., and G. J. Schulz, Rev. Sci. Instrum. 39, 1752 (1968).

Stamatovic, A., and G. J. Schulz, Rev. Sci. Instrum. 41, 423 (1970).

Steele, D., Spectrochima Acta 18, 915 (1962).

Steele, D., and D. H. Whiffen, Spectrochima Acta 16, 368 (1960).

Streets, D. G., and G. P. Ceasar, Mol. Phys. 26, 1037 (1973).

Symons, M. C. R., R. C. Selby, I. G. Smith, and S. W. Bratt, Chem. Phys. Lett. 48, 100 (1977).

Taylor, H. S., G. V. Nazaroff, and A. Golebiewski, J. Chem. Phys. 45, 2872 (1966).

Taylor, P. O., K. T. Dolder, W. E. Kauppila, and G. H. Dunn, Rev. Sci. Instrum. 45, 538 (1974).

VanVeen, E. H., and F. L. Plantenga, Chem. Phys. Lett. 30, 28 (1975).

VanVeen, E. H., and F. L. Plantenga, Chem. Phys. Lett. 38, 493 (1976).

VanVeen, E. H., and F. L. Plantenga, Chem. Phys. Lett. 41, 535 (1976).

VanVeen, E. H., and F. L. Plantenga, Chem. Phys. Lett. 41, 540 (1976).

VonNiessen, W., G. H. F. Diercksen, and L. S. Cederbaum, Chem. Phys. Lett. 45, 295 (1977).

Wong, S. F., and G. J. Schulz, Phys. Rev. Lett. 35, 1429 (1975).

Yim, M. B., and B. E. Wood, J. Am. Chem. Soc. 98, 2053 (1976).

Ziesel, J. P., I. Nenner, and G. J. Schulz, J. Chem. Phys. 63, 1943 (1975).

VITA

John Ronald Frazier was born in Scott County, Virginia on October 12, 1948. He attended elementary schools in that county and was graduated from Gate City High School in May 1966. The following September he entered Berea College, Berea, Kentucky, and in May 1970, he received a Bachelor of Arts degree in Physics.

After a two-year tour of duty with the United States Army, he entered the Graduate School of the University of Tennessee in June 1972. He was awarded an AEC Fellowship in Radiation Science and Protection for his first year of graduate study. Following this, he was a graduate teaching assistant at the University of Tennessee while pursuing a Master of Science degree. This degree was awarded in December 1973. He received the Doctor of Philosophy degree with a major in Physics in March 1978.

He is a member of Sigma Pi Sigma Physics honor society.

Mr. Frazier is presently employed with the Department of Health, Education and Welfare in the Bureau of Radiological Health in Rockville, Maryland.

He is married to the former Patricia Peters of Berea, Kentucky, and has two children, John Michael, age seven, and Amanda Leigh, age one.